

Time-varying Mixing Matrix Design for Energy-efficient Decentralized Federated Learning

Xusheng Zhang*, Tuan Nguyen†, and Ting He†

* University of Oxford, Oxford, England, UK. Email: xusheng.zhang@cs.ox.ac.uk

† Pennsylvania State University, University Park, PA, USA. Email: {tmn5319,tinghe}@psu.edu

Abstract—We consider the design of mixing matrices to minimize the operation cost for decentralized federated learning (DFL) in wireless networks, with focus on minimizing the maximum per-node energy consumption. As a critical hyperparameter for DFL, the mixing matrix controls both the convergence rate and the needs of agent-to-agent communications, and has thus been studied extensively. However, existing designs mostly focused on minimizing the communication time, leaving open the minimization of per-node energy consumption that is critical for energy-constrained devices. This work addresses this gap through a theoretically-justified solution for mixing matrix design that aims at minimizing the maximum per-node energy consumption until convergence, while taking into account the broadcast nature of wireless communications. Based on a novel convergence theorem that allows arbitrarily time-varying mixing matrices, we propose a multi-phase design framework that activates time-varying communication topologies under optimized budgets to trade off the per-iteration energy consumption and the convergence rate while balancing the energy consumption across nodes. Our evaluations based on real data have validated the efficacy of the proposed solution in combining the low energy consumption of sparse mixing matrices and the fast convergence of dense mixing matrices.

Index Terms—Decentralized federated learning, mixing matrix design, energy consumption.

I. INTRODUCTION

Decentralized federated learning (DFL) [1] is an emerging machine learning paradigm that allows distributed learning agents to collaboratively learn a shared model from the union of their local data without directly sharing the data. Instead of coordinating through a parameter server as in centralized federated learning (FL) [2], the agents participating in DFL directly exchange model updates with their neighbors through peer-to-peer communications, which are then aggregated locally [3]. DFL has attracted significant attention since its introduction, because compared to its centralized counterpart, DFL has better robustness by avoiding a single point of failure and better balances the communication loads across nodes without increasing the computational complexity [1].

Meanwhile, DFL still faces significant performance challenges due to the extensive data transfer between learning agents. Such challenges are particularly prominent for deep learning due to the large model size, where communication cost can dominate the total cost of the learning task [4], particularly in resource-constrained edge networks [5]. This

issue has attracted tremendous research interests in reducing the communication cost of DFL, such as methods for reducing the amount of data per communication through compression (e.g., [6]) and methods for reducing the number of communications through hyperparameter optimization (e.g., [7]) or adaptive communications (e.g., [8]).

In particular, the design of *mixing matrix* used for local parameter aggregation plays a crucial role, as each non-zero off-diagonal entry in the mixing matrix will trigger an agent-to-agent communication. In this regard, most existing works focused on accelerating learning by minimizing the communication time, either measured in the maximum number of neighbors an agent communicates with [9], [7], [10], [11] or the number of time slots for scheduling all the communications [12]. However, in wireless networks such as HetNets [5], device-to-device networks [13], and IoT networks [14], an often more important cost measure is energy consumption, which has received less attention. Only a few works have tried to optimize energy consumption during DFL [7], [15], but they either did not consider the balance of energy consumption between nodes [7] or did not utilize the broadcast nature of wireless communications [15].

In this work, we aim at filling this gap with the objective of *minimizing the maximum energy consumption per node* for DFL to reach a given level of convergence, while taking into account the broadcast nature of wireless communications. Our solution is built upon a novel convergence theorem under time-varying mixing matrices, based on which we propose a multi-phase mixing matrix design framework together with concrete algorithms that designs randomized mixing matrices under optimized per-node budgets to optimally balance the convergence rate and the energy consumption at each node.

A. Related Works

Decentralized federated learning. First explored by [1] through Decentralized Parallel Stochastic Gradient Descent (D-PSGD), DFL removes the central server in [2] and enables model training over peer-to-peer networks. A central research question is how DFL performs compared to centralized FL, particularly in convergence rate, communication cost, and generalization. Subsequent studies including [16], [17], [18] advance DFL in both algorithms and theories, though the main focus remains on reducing the number of iterations needed for convergence.

Research was partly supported by the National Science Foundation under award CNS-2106294.

Communication cost reduction. As model sizes continue to grow, communication overhead has become a key bottleneck limiting the performance and reliability of DFL on wireless edge networks [19]. Existing work for reducing communication cost can be broadly categorized into three approaches. The first is to lower the cost per communication round using compression techniques [6], [20], [21], [22]. The second is to reduce the total number of communication rounds [23], [24], [25], [26]. A third line of work focuses on activating only selected subsets of links rather than all links simultaneously. In this direction, event-triggered mechanisms were introduced in [8], [27], and optimized (possibly randomized) communication patterns were proposed in [9], [7], [12].

In this work, we aim at designing the communication patterns as in [9], [7], [12], which has the advantage of providing predictable performance compared to event-triggered mechanisms, but *we consider a different objective*. While most existing works on communication design focused on minimizing the communication time, measured by the number of matchings [9], [7], the maximum degree [10], [11], or the number of collision-free transmission slots [12], we focus on minimizing the maximum energy consumption per node, which is critical for wireless networks [5], [13], [14]. Compared to the communication time, fewer works have tackled the optimization of energy consumption [7], [15], [28], and the existing solutions either ignored the balance of energy consumption across nodes [7] or ignored the broadcast nature of wireless communications [15]. Some solution [28] even ignored the energy consumption by communications. *This work aims at filling this gap by designing the communication patterns to minimize the maximum energy consumption per node, while considering broadcast communications.* While a few works considered broadcast-based DFL [29], [12], they had different optimization objectives (e.g., maximizing #successful links [29] or minimizing #transmission slots [12]).

Mixing matrix design in DFL. The mixing matrix, i.e., the matrix containing the local aggregation weights, is an important hyperparameter in DFL. The impact of the mixing matrix on the convergence rate of DFL is usually captured through its spectral gap [1], [30], [31] or an equivalent parameter that denotes the discrepancy between the designed mixing matrix and the ideal mixing matrix under all-to-all communications [9]. Although recent studies have pointed out additional parameters that can affect convergence, such as the effective number of neighbors [32] and the neighborhood heterogeneity [11], these results do not invalidate the importance of the spectral gap. Based on the identified convergence parameters, several mixing matrix designs have been proposed to balance the convergence rate and the cost per iteration [9], [7], [12], [10], [11]. In this regard, our mixing matrix design is also based on a parameter related to the spectral gap, but *we build on a generalized convergence theorem allowing time-varying mixing matrices* (including random matrices with time-varying distributions), which enables a multi-phase design.

DFL over time-varying topology. Most gossip-based distributed optimization algorithms have been analyzed under

fixed network topologies, with only a few works establishing convergence guarantees for time-varying topologies. [33] studies D-PSGD with multiple steps of local training and multiple steps of gossip, which can be viewed as periodically alternating between the full base topology and an empty topology. [34] provides the state-of-the-art convergence analysis for D-PSGD with very general (randomized) mixing matrices, subject only to a spectral condition in each period. Algorithm subgradient-push [35] also handles time-varying topologies, but their convergence analyses rely on convexity of the loss functions and additional spectral assumptions on the mixing matrices. Gradient tracking algorithms such as DIGing [36] and Acc-GT [37] have likewise been studied over time-varying topologies under convex loss functions. The convergence analysis in [38] is the most general to date, applicable to a broad class of algorithms, requiring neither convexity nor strong assumptions on the topology class; however, it still assumes a uniform lower bound on the spectral gap of the time-varying topologies, an assumption not made in this paper. *The convergence theorem presented here focuses on D-PSGD and applies to topologies with arbitrarily time-varying spectral gaps, covering both convex and non-convex objectives.*

Adaptive communications. Adapting communications during training, e.g., via adapting the communicated content (e.g., adaptive model compression [39], [40], adaptive model pruning [41], adaptive self-distillation [42], [43], adaptive parameter freezing [44]) or the act of communication (e.g., adapting communication period [45], adapting client selection [46], adapting topology construction [47], and adapting both communication period and topology [48]), has been shown to improve the performance of FL. Among these studies, only [47], [48] address decentralized federated learning (DFL), the setting we study here. Their adaptive mechanisms, however, come with non-trivial computational overhead or system complexity: [47] integrates real-time deep reinforcement learning at every iteration, while [48] relies on a central coordinator to compute complicated adaptive decisions. Moreover, the resulting adaptations depend on real-time decisions, and thus the behavior would be difficult to predict or analyze. Our approach moves in a different direction. Based on a generalized convergence theorem, we can *analytically characterize the impact of fine-grained adaptations of the act of communication*, without requiring real-time algorithmic decision-making (from a centralized orchestration), and our method remains compatible with content-level adaptations for further performance gains.

B. Summary of Contributions

We consider the mixing matrix design for broadcast-based DFL, with the objective of minimizing the maximum per-node energy consumption, with the following contributions:

- 1) Motivated by our initial experiments that suggest the benefit of varying the communication intensity during training, we derive a new convergence theorem that allows *arbitrarily time-varying* (random) mixing matrices, which generalizes existing convergence theorems that require mixing matrices

to be fixed [1], i.i.d. [9], B -connected [35], or periodic [34], [33].

2) Based on the theorem, we propose a multi-phase design framework as well as a corresponding trilevel optimization algorithm, and derive explicit expressions of its objective function in the cases of 1-phase and 2-phase design.

3) We develop a budgeted mixing matrix design algorithm to solve the lower-level optimization under broadcast communications, and analytically characterize the convergence rate under its design in the case of fully connected base topology.

4) We evaluate the proposed solution against baselines and state-of-the-art benchmarks under realistic settings for learning in wireless networks. Our results validate the efficacy of the proposed solution in combining the low energy consumption of sparse mixing matrices and the fast convergence of dense mixing matrices to improve the energy efficiency of DFL.

Roadmap. Section II states the problem formulation, Section III presents our convergence theorem, based on which Sections IV–V develop the proposed solution, Section VII presents the performance evaluation, and Section VIII concludes the paper. **All proofs are deferred to the appendix.**

II. BACKGROUND AND PROBLEM FORMULATION

A. Decentralized Learning Problem

Consider a network of m nodes linked via a base topology $G = (V, E)$, where V is the set of nodes ($|V| = m$) and E indicates which node pairs can exchange information directly. That is, each node i can only directly communicate with nodes in its one-hop neighborhood (including itself), denoted by $V_i := \{i\} \cup \{j \in V : (i, j) \in E\}$. Each node $i \in V$ is associated with a local objective function $F_i(\mathbf{x})$, which is a function of the parameter $\mathbf{x} \in \mathbb{R}^d$ that depends on the local dataset at node i . The objective of DFL is to collaboratively minimize the global function

$$F(\mathbf{x}) := \frac{1}{m} \sum_{i=1}^m F_i(\mathbf{x}), \quad (1)$$

which averages the local objectives across all nodes. We assume that F attains its minimum value F_{\inf} .

B. Decentralized Learning Algorithm

We focus on a well-established decentralized learning algorithm known as Decentralized Parallel Stochastic Gradient Descent (D-PSGD) [1]. Let $\mathbf{x}_i^{(t)}$ represent the model parameter at node i at the start of iteration t , and let $g(\mathbf{x}_i^{(t)}; \xi_i^{(t)})$ denote the stochastic gradient computed at that node using a minibatch $\xi_i^{(t)}$ drawn from its local data and the current parameter $\mathbf{x}_i^{(t)}$. At each iteration, D-PSGD performs the following update in parallel at every node i :

$$\mathbf{x}_i^{(t+1)} = \sum_{j=1}^m \mathbf{W}^{(t)}[i, j](\mathbf{x}_j^{(t)} - \eta g(\mathbf{x}_j^{(t)}; \xi_j^{(t)})), \quad (2)$$

where $\mathbf{W}^{(t)} = (\mathbf{W}^{(t)}[i, j])_{i, j=1}^m$ is the $m \times m$ mixing matrix used at iteration t , and $\eta > 0$ denotes the learning rate.

Since node i requires communication from node j in iteration t only when $\mathbf{W}^{(t)}[i, j] \neq 0$, the communication pattern

can be controlled by appropriately designing the mixing matrix $\mathbf{W}^{(t)}$. According to [1], the mixing matrix should be *topology-compliant* ($\mathbf{W}^{(t)}[i, j] \neq 0$ only if $(i, j) \in E$) and *symmetric with each row/column summing up to one*¹ in order to ensure feasibility and convergence for D-PSGD.

In general, the mixing matrix $\mathbf{W}^{(t)}$ can be a random matrix drawn from a distribution $\mathcal{W}^{(t)}$ as long as all its realizations satisfy our desired properties, i.e., being topology-compliant and symmetric with row/column sums of 1. In this case, by $\mathbf{E}[\phi(\mathbf{W}^{(t)})]$ we denote the expectation of a function ϕ of $\mathbf{W}^{(t)}$, where $\mathbf{W}^{(t)}$ is drawn from its distribution $\mathcal{W}^{(t)}$.

Let $\bar{\mathbf{x}}^{(t)} := \frac{1}{m} \sum_{i=1}^m \mathbf{x}_i^{(t)}$ denote the learned global model at iteration t (which is a global average of the local models at this iteration). Depending on the shape of the objective function F , there are two widely adopted convergence criteria: for any *required level of convergence* $\epsilon > 0$, we say that D-PSGD has achieved ϵ -convergence if

- $\frac{1}{T} \sum_{t=0}^{T-1} (\mathbf{E}[F(\bar{\mathbf{x}}^{(t)})] - F_{\inf}) \leq \epsilon$ when the local objective functions F_i are convex, or
- $\frac{1}{T} \sum_{t=0}^{T-1} \mathbf{E}[\|\nabla F(\bar{\mathbf{x}}^{(t)})\|^2] \leq \epsilon$ for general (possibly non-convex) F_i .²

The convergence of D-PSGD can be guaranteed under the following assumptions:

- (1) Each local objective function $F_i(\mathbf{x})$ is L -Lipschitz smooth, i.e., for all $\mathbf{x}, \mathbf{x}' \in \mathbb{R}^d$, $\|\nabla F_i(\mathbf{x}) - \nabla F_i(\mathbf{x}')\| \leq L\|\mathbf{x} - \mathbf{x}'\|$, $\forall i \in V$.
- (2) There exist constants $M_1, \hat{\sigma}$ such that $\frac{1}{m} \sum_{i \in V} \mathbf{E}[\|g(\mathbf{x}_i; \xi_i) - \nabla F_i(\mathbf{x}_i)\|^2] \leq \hat{\sigma}^2 + \frac{M_1}{m} \sum_{i \in V} \|\nabla F(\mathbf{x}_i)\|^2$, $\forall \mathbf{x}_1, \dots, \mathbf{x}_m \in \mathbb{R}^d$.
- (3) There exist constants $M_2, \hat{\zeta}$ such that $\frac{1}{m} \sum_{i \in V} \|\nabla F_i(\mathbf{x})\|^2 \leq \hat{\zeta}^2 + M_2 \|\nabla F(\mathbf{x})\|^2$, $\forall \mathbf{x} \in \mathbb{R}^d$.

While the convergence of D-PSGD has also been proved under other assumptions [1], [9], the above assumptions, originally from [34], are more general; see [34] for explanations.

C. Cost Models

We focus on energy consumption as the cost measure. Specifically, we use $c_i(\mathbf{W}^{(t)})$ to denote the energy consumption at node i in an iteration when the mixing matrix is $\mathbf{W}^{(t)}$, which contains two parts: (i) computation energy c_i^a for computing the local stochastic gradient and the local aggregation, and (ii) communication energy for sending the parameter vector at node i to each of its activated neighbors. Under *broadcast communications* where node i can send its parameter vector to all its neighbors through a broadcast transmission, we model the per-iteration energy consumption at node i as

$$c_i(\mathbf{W}^{(t)}) := c_i^a + c_i^b \mathbb{1}(\exists (i, j) \in E : \mathbf{W}^{(t)}[i, j] \neq 0), \quad (3)$$

where c_i^b is the energy consumption per transmission, and $\mathbb{1}(\cdot)$ denotes the indicator function. We say that node i is *activated*

¹In [1], the mixing matrix was assumed to be symmetric and *doubly stochastic* with entries constrained to $[0, 1]$, but we find that all the convergence proofs only required the mixing matrix to be symmetric with each row/column summing up to one.

²In this work, we use $\|\mathbf{a}\|$ to denote ℓ_2 norm if \mathbf{a} is a vector, and spectral norm if \mathbf{a} is a matrix.

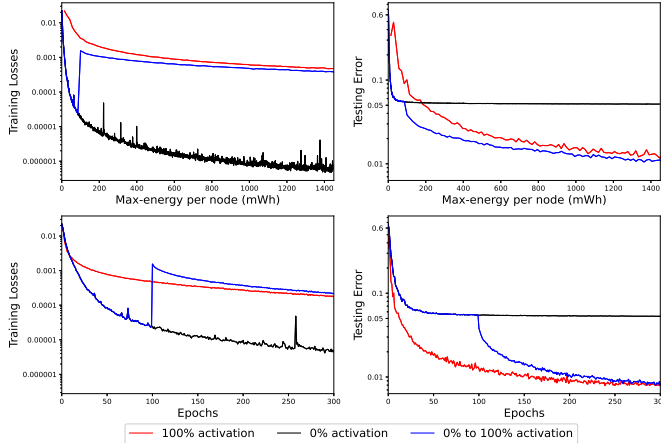


Fig. 1. Motivating experiment based on MNIST over a 100-node clique (x-axis truncated to show the same range for all curves).

in iteration t if $\mathbb{1}(\exists(i,j) \in E : \mathbf{W}^{(t)}[i,j] \neq 0) = 1$. The total energy consumption at node i over T iterations is thus $\sum_{t=1}^T c_i(\mathbf{W}^{(t)})$.

An alternative cost model under *unicast communications* has been studied in [7], [15], where node i needs to separately transmit its parameter vector over each activated link (i,j) with energy consumption c_{ij}^b . In this setting, the energy consumption at node i in iteration t becomes

$$c_i(\mathbf{W}^{(t)}) := c_i^a + \sum_{j:(i,j) \in E} c_{ij}^b \mathbb{1}(\mathbf{W}^{(t)}[i,j] \neq 0). \quad (4)$$

Remark: The above models ignore random factors such as link dynamics and retransmissions, which are left to future work.

D. Design Objective

There is an inherent tradeoff between converging in fewer iterations and spending less energy per iteration, which can be controlled by designing possibly time-varying mixing matrices $(\mathbf{W}^{(t)})_{t=1}^T$. To maximize the lifetime of the learning system, we aim at designing the mixing matrices to *minimize the maximum per-node energy consumption*, defined as

$$\max_{i \in V} \sum_{t=1}^T c_i(\mathbf{W}^{(t)}), \quad (5)$$

until the learning task reaches a required level of convergence.

E. Motivating Experiment

As a motivating example, we compare the tradeoff between learning performance and energy consumption under three example designs. Our experiment is based on the MNIST dataset, randomly distributed across 100 nodes fully connected with each other, each training a 4-layer CNN model with 1,663,370 parameters as in [2], with a batch size of 64 and a learning rate of 0.05. We set the energy consumption parameters as in Section VII. We evaluate the training loss and the testing error under three designs:

- (1) $\mathbf{W}^{(t)} \equiv \frac{1}{m}\mathbf{1}\mathbf{1}^\top$, i.e., all the nodes broadcast their local models in all the iterations ('100% activation'),

- (2) $\mathbf{W}^{(t)} \equiv \mathbf{I}$, i.e., no communication between nodes ('0% activation'), and
- (3) a 2-phase design that starts with \mathbf{I} and switches to $\frac{1}{m}\mathbf{1}\mathbf{1}^\top$ after 100 epochs ('0% to 100% activation').

The trajectories showing training progress as energy is spent, as shown in Fig. 1, suggest that while using a dense mixing matrix yields a lower testing error under high energy budgets, using a sparse mixing matrix is more efficient under low energy budgets due to the savings in communication energy. The low training loss of '0% activation' is due to overfitting, which also explains the initial increase in training loss for the 2-phase design after switching. Suitably switching between the two can achieve a better tradeoff between the quality of learning and the energy consumption than each case alone.

III. CONVERGENCE ANALYSIS

The foundation of our solution is a set of convergence theorems that characterize the number of iterations until convergence as explicit functions of the mixing matrices. To present these theorems, we will need a few notions: the *ideal mixing matrix* $\mathbf{J} := \frac{1}{m}\mathbf{1}\mathbf{1}^\top$ which maintains global consensus, the *divergence* between a designed (possibly random) mixing matrix \mathbf{W} and the ideal mixing matrix defined as

$$\rho(\mathbf{W}) := \|\mathbf{E}[\mathbf{W}^\top \mathbf{W}] - \mathbf{J}\|,$$

and the following parameters that capture the dependence of convergence rate on time-varying mixing matrices.

We define

$$p^{(t)} := 1 - \rho(\mathbf{W}^{(t)}),$$

and let $\mathbf{p} := \{p^{(t)}\}_{t=0}^\infty$. For each $j \geq 0$, define

$$\pi_j := \sum_{i>j} \prod_{t=j+1}^{i-1} \left(1 - \frac{p^{(t)}}{2}\right).$$

The quantity π_j aggregates the contraction effects of time-varying mixing matrices $\{\mathbf{W}^{(t)}\}_{t \geq j+1}$ starting from iteration $j+1$. Each factor $1 - p^{(t)}/2$ upper bounds the amount of divergence at time t , while the product reflects mixing over consecutive iterations accumulated over time. Consequently, π_j provides an upper bound on the cumulative divergence from the averaging operator J that persists after the j -th iteration.

For a time horizon $T > 0$, we further define the time-averaged quantities

$$\Pi_1(T) := \frac{1}{T} \sum_{j=0}^{T-1} \pi_j, \quad \Pi_2(T) := \frac{1}{T} \sum_{j=0}^{T-1} \frac{\pi_j}{p^{(j)}}. \quad (6)$$

The quantity $\Pi_1(T)$ represents the average cumulative divergence over the first T iterations, while $\Pi_2(T)$ is a weighted version that additionally accounts for the instantaneous mixing strength $p^{(j)}$ at the starting time j . Both can be viewed as ergodic measures of how effectively the sequence of time-varying mixing matrices promotes consensus over time.

We collect a few useful facts about the parameters π_j , $\Pi_1(T)$, and $\Pi_2(T)$.

Lemma III.1. Assume there exists $\delta \in (0, 1)$ such that $p^{(t)} \geq \delta$ for all $t \geq 0$. Then the following statements hold:

- 1) For all $j \geq 0$, $\pi_j < \frac{2}{\delta}$.
- 2) For any $T > 0$, $\Pi_1(T) < \frac{2}{\delta}$ and $\Pi_2(T) < \frac{2}{\delta^2}$.
- 3) In particular, if $p^{(t)} \equiv p$, then for any $T > 0$, $\Pi_1(T) = \pi_0 = 2/p$ and $\Pi_2(T) = 2/p^2$.

The following theorem describes how the convergence rate depends on the mixing matrices through the parameters $\Pi_1(T)$, $\Pi_2(T)$, π_0 , and $p_{\min} := \min_j p^{(j)}$.

Theorem III.2. D-PSGD under assumptions (1)–(3) in Section II-B achieves ϵ -convergence (i.e., $\frac{1}{T} \sum_{t=0}^{T-1} \mathbf{E}[\|\nabla F(\bar{\mathbf{x}}^{(t)})\|^2] \leq \epsilon$) when the number of iterations T satisfies $T \geq T_1(\Pi_1(T), \Pi_2(T), \pi_0, p_{\min}, \epsilon, \bar{\mathbf{x}}^{(0)})$ for

$$\begin{aligned} T_1(\Pi_1, \Pi_2, \pi_0, p_{\min}, \epsilon, \bar{\mathbf{x}}^{(0)}) := & O\left(\frac{f_0 L \sqrt{(1+M_1)(1+M_2)}}{\epsilon p_{\min}}\right) \\ & + O\left(\frac{f_0 L^2 [(1+\pi_0)\Xi_0 + (1+M_1)]}{\epsilon}\right) \\ & + f_0 L \cdot O\left(\frac{\hat{\sigma}^2}{m\epsilon^2} + \frac{\sqrt{(M_1\hat{\zeta}^2 + \hat{\sigma}^2)\Pi_1 + \hat{\zeta}^2\Pi_2}}{\epsilon^{3/2}}\right), \end{aligned} \quad (7)$$

where $f_0 := \mathbf{E}[F(\bar{\mathbf{x}}^{(0)})] - F_{\inf}$ (F_{\inf} denotes the minimum value of F) and $\Xi_0 := \frac{1}{m} \sum_{i=1}^m \|x_i^{(0)} - \bar{\mathbf{x}}^{(0)}\|^2$.

The big- O notations used in the Theorem above and throughout the manuscript hide absolute constants independent of all the parameters.

Remark 1: From Theorem III.2, the required number of iterations depends on \mathbf{p} only through $\Pi_1(T)$, $\Pi_2(T)$, π_0 , and p_{\min} . When $p^{(t)} \equiv p$, we have $\Pi_1(T) \equiv 2/p$ and $\Pi_2(T) \equiv 2/p^2$, in which case Theorem III.2 reduces to the state-of-the-art convergence theorem in [34] in the case of $\tau = 1$. Furthermore, with a modified definition of $p^{(t)}$ to characterize τ matrices in consecutive iterations, the proof of Theorem III.2 can be adapted to support the convergence conditions in [34] for general $\tau \geq 1$.

Remark 2: We briefly discuss the contributions of each term in (7). The **third term** is expected to be the dominant one: while the term $O(\hat{\sigma}^2/(m\epsilon^2))$ is asymptotically tight for any stochastic methods [49], [17], the $O(\epsilon^{-3/2})$ part highlights the main novelty in our bound, as it only involves the “average” parameters Π_1 and Π_2 rather than worst-case parameters. The **second term** scales as $O(\epsilon^{-1})$ and depends on π_0 . This dependence is fairly innocuous, especially since one may force $\Xi_0 = 0$ by fixing the same initialization point on all worker nodes; we include such dependence only for completeness. Finally, the **first term** depends on the worst-case parameter p_{\min} in the sequence \mathbf{p} . While this dependence may appear suboptimal, the term itself scales only as $O(\sqrt{M_1 M_2}/\epsilon)$ and is independent of $\hat{\zeta}$ and $\hat{\sigma}$, so its overall impact is not expected to be significant.

Remark 3: Analysis of decentralized gradient-based optimization algorithms with time-varying mixing matrices has

been studied in [35], [36], but their convergence guarantees rely on convexity of F_i ’s and other strong assumptions on both the mixing matrices and the objective functions $\{F_i\}_{i=1}^m$. Our techniques also extend to the convex setting: we establish a convergence theorem analogous to Theorem III.2 showing that the algorithm achieves ϵ -convergence, i.e., $\frac{1}{T} \sum_{t=0}^{T-1} (\mathbf{E}[F(\bar{\mathbf{x}}^{(t)})] - F_{\inf}) \leq \epsilon$, under an additional assumption that the local objectives are convex. Moreover, in this case, our requirements (1)–(3) can be further relaxed; in particular, we may assume $M_1 = M_2 = 0$. See Appendix B for details.

The convergence condition in Theorem III.2 may be satisfied by multiple choices of T . We thus define $T_2(\mathbf{p}, \epsilon, \bar{\mathbf{x}}^{(0)})$ as the smallest T that satisfies the convergence condition for a given sequence \mathbf{p} , error bound ϵ , and initial model $\bar{\mathbf{x}}^{(0)}$, i.e.,

$$\begin{aligned} T_2(\mathbf{p}, \epsilon, \bar{\mathbf{x}}^{(0)}) := & \\ \min\{T > 0 : T \geq T_1(\Pi_1(T), \Pi_2(T), \pi_0, p_{\min}, \epsilon, \bar{\mathbf{x}}^{(0)})\}. \end{aligned} \quad (8)$$

If the local objective functions are convex, we define T_2 analogously as

$$\begin{aligned} T_2(\mathbf{p}, \epsilon, \bar{\mathbf{x}}^{(0)}) := & \\ \min\{T > 0 : T \geq T_4(\Pi_1(T), \Pi_2(T), \pi_0, p_{\min}, \epsilon, \bar{\mathbf{x}}^{(0)})\} \end{aligned} \quad (9)$$

where T_4 denotes the convergence bound given in Theorem A.3.

IV. OPTIMIZATION FRAMEWORK

At a high level, our design objective as stated in Section II-D can be formulated as the following optimization problem:

$$\min_{T, \{\mathbf{W}^{(t)}\}_{t=1}^T} \max_{i \in V} \sum_{t=1}^T c_i(\mathbf{W}^{(t)}) \quad (10a)$$

$$\text{s.t. } T \geq T_2(\mathbf{p}, \epsilon, \bar{\mathbf{x}}^{(0)}), \quad (10b)$$

$$p^{(t)} = 1 - \rho(\mathbf{W}^{(t)}), \quad \forall t = 1, \dots, T. \quad (10c)$$

The design variables include both the number of iterations T and the sequence of mixing matrices $\{\mathbf{W}^{(t)}\}_{t=1}^T$. We treat ϵ and the initial model $\bar{\mathbf{x}}^{(0)}$ as explicit inputs to the formulation.

A. Randomized Multi-phase Design Framework

We note that under broadcast communications, deterministic mixing matrix design is not sufficient. This is because if any iteration t uses a deterministic mixing matrix $\mathbf{W}^{(t)}$ for which the set of communicating nodes U is not equal to V , then $\mathbf{W}^{(t)}$ is a reducible mixing matrix and thus $\rho(\mathbf{W}^{(t)}) = \|\mathbf{W}^{(t)} - J\|^2 = 1$, which implies $\Pi_2(T) = \infty$ and thus the right-hand side of (10b) is infinite. Therefore, any deterministic mixing matrix design must activate communications at all the nodes in all the iterations. Under this constraint, the mixing matrix design problem reduces to the simple problem of designing a single mixing matrix \mathbf{W} with the minimum $\rho(\mathbf{W})$ based on the entire base topology G , whose solution can be rather suboptimal in energy efficiency as shown in Section II-E (‘100% activation’). By employing a randomized mixing matrix design, we can avoid this constraint

and significantly enlarge the design space. Therefore, we generalize the problem from a deterministic design problem (10) to a randomized design problem, by replacing its objective (10a) with

$$\min_{T, \{\mathbf{W}^{(t)}\}_{t=1}^T} \mathbf{E} \left[\max_{i \in V} \sum_{t=1}^T c_i(\mathbf{W}^{(t)}) \right].$$

To simplify the computation, we divide the training process into K *phases*, where K is a design variable. Each phase $s \in \{1, \dots, K\}$ contains τ_s consecutive iterations of using the random mixing matrix \mathbf{W}_s . For clarity, we use $\mathbf{W}_s^{(t)}$ to refer to the mixing matrix used in the t -th iteration of phase s , which is an instance of \mathbf{W}_s drawn independently in each iteration. This changes our design problem into the following optimization:

$$\min_{K, \{\mathbf{W}_s, \tau_s\}_{s=1}^K} \mathbf{E} \left[\max_{i \in V} \sum_{s=1}^K \sum_{t=1}^{\tau_s} c_i(\mathbf{W}_s^{(t)}) \right] \quad (11a)$$

$$\text{s.t. } \tau_1 + \dots + \tau_K = T_2(\mathbf{p}, \epsilon, \bar{\mathbf{x}}^{(0)}) \quad (11b)$$

$$p^{(t)} = 1 - \rho(\mathbf{W}_s), \forall t = \left(\sum_{l=1}^{s-1} \tau_l, \dots, \sum_{l=1}^s \tau_l \right], \quad (11c)$$

$$\forall s = 1, \dots, K.$$

The decision variables are: the number of phases K , the K random mixing matrices $\{\mathbf{W}_s\}_{s=1}^K$, and the number of iterations $\{\tau_s\}_{s=1}^K$ for using each. For a given solution to (11), the number of iterations required for convergence is denoted as

$$T_3((p_1, \tau_1), (p_2, \tau_2), \dots, (p_K)) := T_2(\mathbf{p}, \epsilon, \mathbf{x}^{(0)}), \quad (12)$$

where $p_s := 1 - \rho(\mathbf{W}_s)$ is the convergence parameter for each phase $s = 1, \dots, K$. Note that, given $(p_1, \tau_1), (p_2, \tau_2), \dots, (p_K)$ and K , τ_K is no longer an independent variable due to (11b).

B. A Related Sub-problem

Since $T_3((p_1, \tau_1), \dots, (p_K))$ is a decreasing function of each $p_s = 1 - \rho(\mathbf{W}_s)$, we want to design a random mixing matrix for each phase s to minimize $\rho(\mathbf{W}_s)$ without triggering too many communications. To this end, we introduce a sub-problem of budgeted mixing matrix design. Let $D > 0$ denote the *budget* for the per-iteration expected energy consumption at each node in a given phase. We formulate the per-phase mixing matrix design problem (omitting the phase index) as

$$\min_{\Pr[\cdot]} \left\| \sum_{\mathbf{W} \in \mathcal{M}} \Pr[\mathbf{W}] \mathbf{W}^\top \mathbf{W} - J \right\| \quad (13a)$$

$$\sum_{\mathbf{W} \in \mathcal{M}} \Pr[\mathbf{W}] = 1, \text{ and } \Pr[\mathbf{W}] \geq 0 \quad \forall \mathbf{W} \in \mathcal{M}, \quad (13b)$$

$$\sum_{\mathbf{W} \in \mathcal{M}} \Pr[\mathbf{W}] c_i(\mathbf{W}) \leq D, \forall i \in V \quad (13c)$$

$$\mathbb{1}[\Pr[\mathbf{W}] \cdot \mathbf{W}[i, j] \neq 0] \leq \mathbb{1}[E[i, j] \neq 0], \quad (13d)$$

$$\forall \mathbf{W} \in \mathcal{M}, \forall i \neq j \in V,$$

where we use \mathcal{M} to denote the set of symmetric matrices whose row/column sums are 1, and $\Pr[\mathbf{W}]$ to denote the probability of choosing $\mathbf{W} \in \mathcal{M}$ in each iteration of this phase.

We will dive into a concrete solution to (13) in Section V-VI. To present the overall solution, we assume the existence of a hypothetical solution \mathcal{A} to (13), treated as a black box for the time being, with the following property: for any budget D , \mathcal{A} provides a random mixing matrix \mathbf{W} that is feasible for (13) with the guarantee that there exists a function $\rho_{\mathcal{A}}^+ : \mathbb{R}^+ \rightarrow \mathbb{R}^+ \cup \{\infty\}$ such that $\rho(\mathbf{W}) \leq \rho_{\mathcal{A}}^+(D)$.

Under a given budget D , one can bound the expected maximum energy consumption per node for a phase of T iterations by the following lemma.

Lemma IV.1. Let $D > 0$ and $T > 0$. Suppose a random mixing matrix \mathbf{W} satisfies $\mathbf{E}[c_i(\mathbf{W})] \leq D$ ($\forall i \in V$). If $\mathbf{W}^{(1)}, \dots, \mathbf{W}^{(T)}$ are i.i.d. copies of \mathbf{W} , then

$$\mathbf{E} \left[\max_i \sum_{t=1}^T c_i(\mathbf{W}^{(t)}) \right] \leq D \cdot \left(T + m \sqrt{\frac{T\pi}{8}} \right) =: q(T, D). \quad (14)$$

The proof of Lemma IV.1 is deferred to Section C.

C. Case Studies for $K = 1$ and $K = 2$

1) *Computation of T_3 :* Next we illustrate computation for T_3 through case studies of $K = 1$ and $K = 2$.

In the case of $K = 1$, as explained in the first remark below Theorem III.2, we have $\Pi_1(T) \equiv 2/p_1$ and $\Pi_2(T) \equiv 2/p_1^2$. With this simplification,

$$\begin{aligned} T_3(p_1) &= T_1(2/p_1, 2/p_1^2, 2/p_1, p_1, \epsilon, \bar{\mathbf{x}}^{(0)}) \\ &= O\left(\frac{f_0 L \sqrt{(1+M_1)(1+M_2)}}{\epsilon p_1}\right) \\ &+ O\left(\frac{f_0 L^2 [\Xi_0 + p_1(1+M_1)]}{\epsilon p_1}\right) \\ &+ f_0 L \cdot O\left(\frac{\hat{\sigma}^2}{m\epsilon^2} + \frac{\sqrt{(M_1\hat{\zeta}^2 + \hat{\sigma}^2)p_1 + \hat{\zeta}^2}}{\epsilon^{3/2} p_1}\right). \end{aligned} \quad (15)$$

In the case of $K = 2$, $\Pi_1(T)$ and $\Pi_2(T)$ are given by the following lemma.

Lemma IV.2. Let $T \geq \tau_1$ be a fixed integer. If $p^{(1)} = \dots = p^{(\tau_1)} = p_1$ and $p^{(\tau_1+1)} = \dots = p^{(T)} = p_2$, then $\Pi_1(T)$ and $\Pi_2(T)$ as defined in (6) satisfy the followings:

$$\Pi_1(T) = \frac{2(T - \tau_1)}{Tp_2} + \frac{2\tau_1}{Tp_1} - \left(\frac{2}{Tp_1} - \frac{2}{Tp_2} \right) \sum_{j=1}^{\tau_1} (1 - \frac{p_1}{2})^j,$$

$$\Pi_2(T) = \frac{2(T - \tau_1)}{Tp_2^2} + \frac{2\tau_1}{Tp_1^2} - \left(\frac{2}{Tp_1^2} - \frac{2}{Tp_2 p_1} \right) \sum_{j=1}^{\tau_1} (1 - \frac{p_1}{2})^j.$$

The proof of Lemma IV.2 is elementary and will be provided in Appendix C. From Lemma IV.2 we have $\Pi_1(T) \rightarrow 2/p_2$ and $\Pi_2(T) \rightarrow 2/p_2^2$ as T grows. Therefore, by a linear search over $T = \tau_1, \tau_1 + 1, \dots$, the first T satisfying $T \geq T_1(\Pi_1(T), \Pi_2(T), \pi_0, p_{\min}, \epsilon, \bar{\mathbf{x}}^{(0)})$ is the value of $T_3((p_1, \tau_1), p_2)$.

Algorithm 1: Multi-phase Mixing Matrix Design

input : Maximum #phases \bar{K} , subroutine \mathcal{A} for the problem (13) and an associated function $\rho_{\mathcal{A}}^+$.

output: Mixing matrices $\bigcup_{s=1}^{K^*} \{\mathbf{W}_s^{(t)}\}_{t=1}^{\tau_s^*}$.

1 **for** $K \leftarrow 1$ **to** \bar{K} **do**

2 Minimize $Q_K = \sum_{s=1}^K q(\tau_s, D_s)$ for
 $\tau_K = T_3((p_1, \tau_1), \dots, (p_{K-1}, \tau_{K-1}), p_K) - \sum_{s=1}^{K-1} \tau_s$
 $\text{and } p_s = 1 - \rho_{\mathcal{A}}^+(D_s);$

3 $K^* \leftarrow \arg \min_K Q_K$, with the corresponding solution
 $D_1^*, \dots, D_{K^*}^*, \tau_1^*, \dots, \tau_{K^*-1}^*;$

4 **for** $s \leftarrow 1$ **to** K^* **do**

5 **for** $t \leftarrow 1$ **to** τ_s^* **do**

6 $\mathbf{W}_s^{(t)} \leftarrow \mathcal{A}(D_s^*);$

7 **return** $\bigcup_{s=1}^{K^*} \{\mathbf{W}_s^{(t)}\}_{t=1}^{\tau_s^*};$

2) *Computation of Design Objective:* Lemma IV.1 together with the function $\rho_{\mathcal{A}}^+(D)$ enables us to upper-bound the objective function (11a). As an example, consider $K = 1$. By Lemma IV.1, the random mixing matrix \mathbf{W} designed by \mathcal{A} for budget D will achieve convergence with an expected maximum energy consumption per node no more than

$$Q_{K=1}(D) := q(T_3(1 - \rho_{\mathcal{A}}^+(D)), D). \quad (16)$$

Thus, by relaxing the objective function (11a) into its upper bound (16), we can obtain a 1-phase (randomized) mixing matrix design by minimizing $Q_{K=1}(D)$ over $D \in \mathbb{R}^+$ and then feeding the resulting D into the given subroutine \mathcal{A} to obtain a random mixing matrix \mathbf{W} .

Now consider the case of $K = 2$. This enlarges our design space to include distinct positive budgets $D_1 > 0$ and $D_2 > 0$ for each phase, as well as the number of iterations τ_1 for phase 1. We first rewrite the objective function (11a) specific to $K = 2$:

$$\begin{aligned} \min_{\{\mathbf{W}_s, \tau_s\}_{s=1}^K} \mathbf{E} \left[\max_{i \in V} \sum_{s=1}^K \sum_{t=1}^{\tau_s} c_i(\mathbf{W}_s^{(t)}) \right] = \\ \min_{\mathbf{W}_1, \mathbf{W}_2, \tau_1} \mathbf{E} \left[\max_{i \in V} \left[\sum_{t=1}^{\tau_1} c_i(\mathbf{W}_1^{(t)}) + \sum_{t=\tau_1+1}^{T_3((p_1, \tau_1), p_2)} c_i(\mathbf{W}_2^{(t-\tau_1)}) \right] \right] \end{aligned} \quad (17)$$

Given a solution \mathcal{A} to the sub-problem (13), we apply \mathcal{A} to D_1 and D_2 , respectively. Then, based on the performance bound $\rho_{\mathcal{A}}^+$, the objective (17) of 2-phase design can be upper-bounded by

$$Q_{K=2}(D_1, D_2, \tau_1) := q(\tau_1, D_1) + q(T_3((p_1, \tau_1), p_2) - \tau_1, D_2), \quad (18)$$

where $p_1 = 1 - \rho_{\mathcal{A}}^+(D_1)$ and $p_2 = 1 - \rho_{\mathcal{A}}^+(D_2)$. Therefore, optimizing $Q_{K=2}(D_1, D_2, \tau_1)$ over the 3-tuple (D_1, D_2, τ_1) will yield an optimized 2-phase design.

D. Overall Solution

We propose to solve the multi-phase design problem (11) through a trilevel optimization as shown in Algorithm 1:

- **Upper-level optimization:** Decide the number of phases K to minimize the overall objective.

Algorithm 2: Budgeted Mixing Matrix Design for Broadcast Communication

Input: A base topology $G = (V, E)$ with per-computation cost c_i^a and per-transmission cost c_i^b ($\forall i \in V$) and per-node budget D .

Output: A mixing matrix \mathbf{W} with an expected per-node cost no more than D .

1 **Step 1: Sample a subset of nodes to activate**

2 Let $U \leftarrow \emptyset$ denote the set of activated nodes;

3 **foreach** $i \in V$ **do**

4 Add node i to U independently with probability
 $\min((D - c_i^a)/c_i^b, 1);$

5 **Step 2: Design entries for nodes not in U**

6 **foreach** $i \in V \setminus U$ **do**

7 $\mathbf{W}[i, i] \leftarrow 1;$

8 $\mathbf{W}[i, j] \leftarrow 0$, $\mathbf{W}[j, i] \leftarrow 0$ for all $j \neq i$;

9 **Step 3: Design entries for nodes in U**

10 **foreach** $i \in U$ **do**

11 **foreach** $j \in U \setminus V_i$ **do**

12 $\mathbf{W}[i, j] \leftarrow 0;$

13 **foreach** $j \in (V_i \cap U) \setminus \{i\}$ **do**

14 $\mathbf{W}[i, j] \leftarrow 1/\max(|V_i \cap U|, |V_j \cap U|);$

15 $\mathbf{W}[i, i] \leftarrow 1 - \sum_{j \in V \setminus \{i\}} \mathbf{W}[i, j];$

- **Intermediate-level optimization:** Given a number of phases K , minimize the relaxed objective $Q_K := \sum_{s=1}^K q(\tau_s, D_s)$ to determine the budget D_s and the duration τ_s of each phase $s = 1, \dots, K$.
- **Lower-level optimization:** Given the budget D_s of each phase, design a random instance $\mathbf{W}_s^{(t)}$ of the mixing matrix for each iteration in this phase by applying the given solution to the sub-problem (13).

The focus of Algorithm 1 is on the intermediate-level optimization, which optimizes a function of $2K - 1$ variables (i.e., $D_1, \dots, D_K, \tau_1, \dots, \tau_{K-1}$). Given the performance bound $\rho_{\mathcal{A}}^+$ of the lower-level optimization, this intermediate-level optimization only has an $O(K)$ -dimensional solution space, which is much more tractable than directly optimizing $K m \times m$ random matrices.

Remark: In the remainder of this work, we will solve the upper/intermediate-level optimizations numerically for small values of K to focus on solving the lower-level optimization under broadcast communications. Our trilevel optimization framework is generally applicable under any communication model. We leave the development of more efficient solutions to the upper/intermediate-level optimizations to future work.

V. LOWER-LEVEL OPTIMIZATION UNDER BROADCAST COMMUNICATION

In this section, we focus on developing efficient solutions to the budgeted problem defined in (13) under the broadcast communication cost model.

A. Algorithm Design

To pose a well-defined and non-trivial problem, we assume

$$\max_i c_i^a \leq D < \max_i (c_i^a + c_i^b). \quad (19)$$

Indeed, if $D \geq \max_i(c_i^a + c_i^b)$, then we can deterministically activate all the nodes, in which case the optimal mixing matrix can be efficiently computed by solving a semi-definite programming problem [7]. Meanwhile, $D < \max_i c_i^a$ is not feasible under the cost model in (3) as some node will exceed the budget even if it does not communicate.

Under the cost model (3), the problem (13) becomes

$$\min_{\Pr[\cdot]} \left\| \sum_{\mathbf{W} \in \mathcal{M}} \Pr[\mathbf{W}] \mathbf{W}^\top \mathbf{W} - \mathbf{J} \right\| \quad (20a)$$

$$\sum_{\mathbf{W} \in \mathcal{M}} \Pr[\mathbf{W}] = 1, \text{ and } \Pr[\mathbf{W}] \geq 0 \quad \forall \mathbf{W} \in \mathcal{M}, \quad (20b)$$

$$c_i^a + \Pr[\exists j \neq i : \mathbf{W}[i, j] \neq 0] \cdot c_i^b \leq D, \quad \forall i \in V \quad (20c)$$

$$\Pr[\mathbb{1}[\mathbf{W}[i, j] \neq 0] \leq \mathbb{1}[E[i, j] \neq 0], \forall i \neq j \in V] = 1. \quad (20d)$$

We now present Algorithm 2, a randomized algorithm designed to solve (20) in 3 steps.

- 1) In Step 1, we activate a subset of nodes $U \subseteq V$ by independently selecting each node with a probability reflecting its residual budget after subtracting the computation cost.
- 2) In Step 2, nodes in $V \setminus U$ are assigned weights so that they essentially perform only local updates.
- 3) In Step 3, nodes in U are assigned mixing weights between themselves according to the Metropolis–Hastings rule [50].

Random client selection—as used in Step 1 of Algorithm 2—has been a standard technique in centralized FL to improve communication efficiency [2], [51]. In the decentralized setting, SwarmSGD [52] can be viewed as a special case of our random client selection in which only two randomly chosen adjacent nodes gossip. The method in [53] adopts a similar strategy of keeping one random neighbor for each node, but further refines it by optimizing the sampling distribution to favor high-speed edges. Our random-selection, in contrast, places no restrictions on the number of participating nodes or the number of neighbors each node may have, yet it guarantees that every realization yields a mixing-matrix design tailored to our specific budgeted problem. In particular, in Lemma V.1 we show that the mixing matrix generated by Algorithm 2 is always topology-compliant and a feasible solution to problem (20), e.g., a valid randomized mixing matrix that satisfies the budget D at every node.

Lemma V.1. Let G be an arbitrary base topology. Assume (19) holds for the given $(c_i^a, c_i^b)_{i \in V}$ and D . The mixing matrix \mathbf{W} outputted by Algorithm 2 is a feasible solution to problem (20).

B. Performance Analysis

1) *Result for Fully-connected Base Topology:* Consider the case where the base topology is a clique, i.e., every node can receive the broadcast of every other node³. In this case, we can characterize the performance of Algorithm 2 analytically.

³We assume that proper transmission scheduling is in place to avoid collision. The specific schedule is irrelevant under the cost model (3).

To present this result, we introduce some additional notations. We use \sim_m to relate two quantities A and B if $\lim_{m \rightarrow \infty} \frac{A}{B} = 1$, that is, A is *asymptotically equivalent* to B . Also, for each $i \in V$, we let

$$\omega_i := \min \left(\frac{D - c_i^a}{c_i^b}, 1 \right),$$

and we use ω to denote the vector $[\omega_1, \omega_2, \dots, \omega_m]$. Lastly, given an arbitrary vector \mathbf{a} , let $\text{diag}(\mathbf{a})$ denote the diagonal matrix with \mathbf{a} on the main diagonal, and \mathbf{a}^2 denote the vector $[a_1^2, \dots, a_m^2]$. Based on these notations, we characterize the performance of Algorithm 2 as follows.

Theorem V.2. Assume G is a clique, and (19) holds for the given cost vectors $(c_i^a, c_i^b)_{i \in V}$ and budget parameter D . The mixing matrix \mathbf{W} designed by Algorithm 2 satisfies

$$\rho(\mathbf{W}) \sim_m \|m^\perp \omega \omega^\top + \text{diag}(\mathbf{1} - \omega) - \mathbf{J}\|, \quad (21)$$

where m^\perp denote the scalar $\mathbf{E}[\frac{1}{|U|} \mid U \neq \emptyset]$ with the expectation taken over the random generation of U .

Moreover, in the special case of homogeneous cost parameters, i.e., $c_i^a \equiv c^a$, $c_i^b \equiv c^b$, we can explicitly express the dependency of $\rho(\mathbf{W})$ on the cost parameters (c^a, c^b) and the budget D . Specifically, for any D satisfying $c^a \leq D < c^a + c^b$, we have

$$\omega_i = \frac{D - c^a}{c^b} =: \tilde{\omega}, \quad \forall i \in V.$$

Given the fact that $m^\perp \sim_m 1/(\tilde{\omega}m)$, we obtain that

$$\begin{aligned} \rho(\mathbf{W}) &\sim_m \left\| \frac{1}{\tilde{\omega}m} \cdot \tilde{\omega}^2 \mathbf{1} \mathbf{1}^\top + (1 - \tilde{\omega}) \mathbf{I} - \mathbf{J} \right\| \\ &= \|(1 - \tilde{\omega})(\mathbf{I} - \mathbf{J})\| = 1 - \tilde{\omega} = 1 - \frac{D - c^a}{c^b}. \end{aligned} \quad (22)$$

2) *Discussion on General Base Topology:* Using a similar analysis as Theorem V.2, one could derive an analogous bound on $\rho(\mathbf{W})$ for the \mathbf{W} designed by Algorithm 2. However, the bound will involve $O(m^2)$ conditional expectations analogous to m^\perp , which is challenging to compute numerically. In this case, we evaluate $\rho(\mathbf{W})$ numerically through Monte Carlo experiments, i.e., for a given budget D , we generate a large number of matrices $\mathbf{W}_1, \dots, \mathbf{W}_N$ from independent runs of Algorithm 2 and use the empirical mean

$$\hat{\rho}(\mathbf{W}) = \left\| \frac{1}{N} \sum_{n=1}^N \mathbf{W}_n^\top \mathbf{W}_n - \mathbf{J} \right\|$$

to approximate $\rho(\mathbf{W})$.

VI. LOWER-LEVEL OPTIMIZATION UNDER UNICAST COMMUNICATION

For the budgeted problem in (13) to be feasible and non-trivial under the unicast cost model (4), we assume

$$\max_i c_i^a \leq D < \max_i \left(c_i^a + \sum_{j:(i,j) \in E} c_{ij}^b \right). \quad (23)$$

This section presents a (meta-)algorithm for solving (13) for any budget D that satisfies the condition in (23), on a general base topology $G = (V, E)$ with arbitrary cost vectors $(c_i^a, c_{ij}^b)_{(i,j) \in E}$.

A. Meta-algorithm Design

The algorithm starts by employing a random graph oracle to sample subgraph of the base topology G as candidate topologies, with which we then compute an optimal distribution over the candidates using semi-definite programming (SDP). Random candidates are iteratively added until the mixing rate objective reaches a convergence threshold. See Algorithm 3 for its pseudo-code.

Algorithm 3: Budgeted Mixing Matrix Design for Unicast Communication

Input: A base topology $G = (V, E)$ with per-computation cost c_i^a and per-transmission cost c_{ij}^b ($\forall i, j \in V$) and per-node budget D ; a random graph oracle \mathcal{G}_G ; a convergence threshold parameter $\delta > 0$.

Output: A list of mixing matrices with their probabilities $\{(\mathbf{W}_s, p_s)\}_{s=0}^k$.

1 Let $\rho_0 \leftarrow 1$;
 2 Let $k \leftarrow 0$ and $\mathbf{W}_0 = I$;
 3 **repeat**
 4 $k \leftarrow k + 1$;
 5 Draw $G_k = (V_k, E_k)$ from \mathcal{G}_G ;
 6 **foreach** $(u, v) \in E_k$ **do**
 7 Let $A_k[u, v] = 1 / \max(\deg_{G_k}(u), \deg_{G_k}(v))$;
 8 Set $D_k[u, u] = \sum_v A_k[u, v]$;
 9 Set $L_k = D_k - A_k$ and $\mathbf{W}_k = I - L_k$;
 10 Given k candidate matrices $(\mathbf{W}_0, \mathbf{W}_1, \dots, \mathbf{W}_k)$,
 11 solve (24) for the optimal probability vector
 12 (p_0, p_1, \dots, p_k) and denote its objective value by
 13 ρ_k ;
 14 **until** $|\rho_k - \rho_{k-1}| < \delta$ and $\rho_k < 1$;
 15 Return $\{(\mathbf{W}_s, p_s)\}_{s=0}^k$;

It can be verified that the output of Algorithm 3 is a feasible solution to the problem defined in (13). Specifically, at Line 10 in each iteration k , we solve the optimization problem given in (24). A straightforward calculation shows that the objective (24a) is equivalent to (13a). Moreover, the budget constraint in (24c) is a direct instantiation of (13c) under the unicast cost model. Finally, the random graph oracle \mathcal{G}_G ensures that each sampled graph G_k is a subgraph of G , thereby automatically

satisfying the constraint (13d).

$$\min_{p_0, \dots, p_k} \left\| \sum_{h=0}^k p_h \mathbf{W}_h^\top \mathbf{W}_h - J \right\| \quad (24a)$$

$$\sum_{h=0}^k p_h = 1 \quad \text{and} \quad p_h \geq 0 \quad \forall h = 0, \dots, k \quad (24b)$$

$$c_i^a + \sum_{h=0}^k p_h \sum_{j:(i,j) \in E_h} c_{ij}^b \leq D, \quad \forall i \in V. \quad (24c)$$

Problem (24) is similar to problem (19) in [7], with the key difference that constraint (24c) imposes a “per-node cost constraint”, whereas the latter enforces a total cost constraint. In each iteration, we solve an instance of (24) with an increasing value of k . Each instance is a linear SDP and can therefore be solved in polynomial time with respect to #matrices k and #nodes m . Since the optimal solution from iteration $k-1$ remains feasible for iteration k , the objective value ρ_k is non-increasing. Assume that the random oracle guarantees $\rho_k < 1$ within at most $O(m)$ iterations, a property that can be verified for every oracle we consider for a sufficiently large D ; see Lemma VI.2. Once $\rho_k < 1$, there are two possibilities:

- If ρ_k decreases by at least δ in every iteration, then the algorithm terminates after at most $O(1/\delta)$ iterations.
- Otherwise, the algorithm stops at some iteration k^* where the improvement becomes negligible, i.e.,

$$|\rho_{k^*} - \rho_{k^*-1}| < \delta.$$

Therefore, the total running time of Algorithm 3 is polynomial in #nodes m and δ^{-1} .

Algorithm 3 provides a unified framework that encompasses the approaches proposed in several prior works. Each of these algorithms can be implemented using Algorithm 3, equipped with different random graph oracles and suitably modified optimization objectives:

- [9] and [54] introduce Matching Decomposition Sampling, which optimizes the distribution over sets of matchings.
- [7] proposes Laplacian Matrix Sampling, which computes an optimal distribution over a set of (spectral) sparsifiers;
- [12] presents BASS, which designs a distribution over collision-free subgraphs to accelerate communication.

For our unicast cost model, we propose to use the following random graph generator: first, in each iteration k draw a random regular graph H_k with degree

$$d := \min_i \frac{D - c_i^a}{\max_j c_{ij}^b};$$

then let $G_k = (V, E \cap E(H_k))$.

B. Performance Analysis

1) *Complete Base Topology:* When the base topology G is a clique, the random graph oracle effectively produces *Ramanujan graphs* [55]. The choice of degree ensures that each Ramanujan graph satisfies the maximum per-node budget

constraint. In addition, the work in [15] establishes an upper bound on $\rho(\mathbf{W})$ when \mathbf{W} is a deterministic mixing matrix defined over a fixed Ramanujan graph. Therefore, when Algorithm 3 is equipped with this oracle, it constructs a randomized mixing matrix by optimizing a distribution over multiple such Ramanujan graphs — resulting in performance that is at least as good as the individual graphs, if not better. As a consequence, the upper bound established for the deterministic case directly extends to our algorithm.

Corollary VI.1. Assume G is a clique, and (23) holds for the given cost vectors $(c_i^a, c_{ij}^b)_{(i,j) \in E}$ and budget D . The mixing matrix \mathbf{W} designed by Algorithm 3 when equipped with a Ramanujan graph generator as the oracle \mathcal{G}_G satisfies

$$\rho(\mathbf{W}) \leq \frac{4}{d} = \max_i \frac{4 \max_j c_{ij}^b}{D - c_i^a},$$

regardless of #iterations k (i.e., valid even if $k = 1$).

2) *General Base Topology:* In the general setting with an arbitrary cost vector and base topology G , Algorithm 3 is expected to perform well because it addresses heterogeneity in two ways: the weight setting used in Line 7 helps absorb structural imbalances in G , while the optimization over a distribution of graphs allows the algorithm to adapt to variations in the cost vector. These two components together enable the construction of a randomized mixing matrix with favorable spectral properties. In practice, since analytically bounding $\rho(\mathbf{W})$ is difficult, we use the empirical estimate of $\rho(\mathbf{W})$ as a practical surrogate for $\rho_{\mathcal{A}}^+$ in the intermediate-level optimization.

Moreover, as observed in [15], finding a deterministic matrix \mathbf{W} for a general graph that satisfies the maximum per-node budget constraint and achieves $\rho(\mathbf{W}) < 1$ is NP-hard under the unicast cost model. In contrast, if the problem is relaxed to allow \mathbf{W} to be a randomized matrix as considered here, then under the corresponding budget constraint (24c), the problem becomes tractable. Specifically, Lemma VI.2 guarantees that in Algorithm 3, $\rho_k < 1$ happens within $O(m)$ iterations with high probability.

Lemma VI.2. Suppose $G = (V, E)$ is a connected graph, and assume that there exists $c > 0$ such that for each $e \in E$, $G_k \sim \mathcal{G}_G$ contains e with probability at least c . Let τ be the first iteration k when $\rho_k < 1$. With probability $1 - e^{-\Omega(m)}$, we have $\tau = O(m/c)$.

VII. PERFORMANCE EVALUATION

We evaluate the proposed solution against benchmarks on a real dataset under realistic settings.

A. Evaluation Setting

1) *Problem Setting:* We consider the standard task of image classification based on CIFAR-10, which consists of 60,000 color images in 10 classes. We train a lightweight version of ResNet-50 with 1.5M parameters over its training dataset with 50,000 images, and then test the trained model over the testing dataset with 10,000 images. We set the learning rate to 0.01,

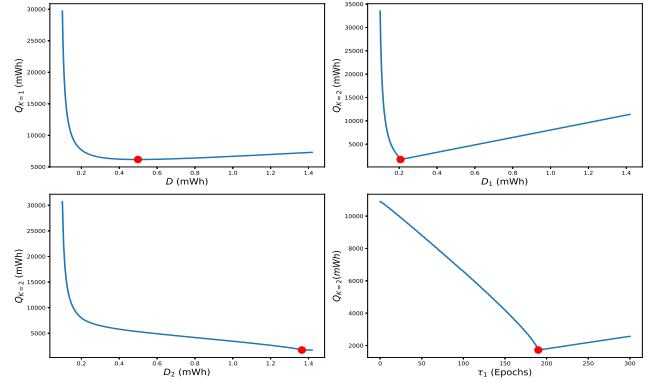


Fig. 2. Design objective vs. design parameters for clique.

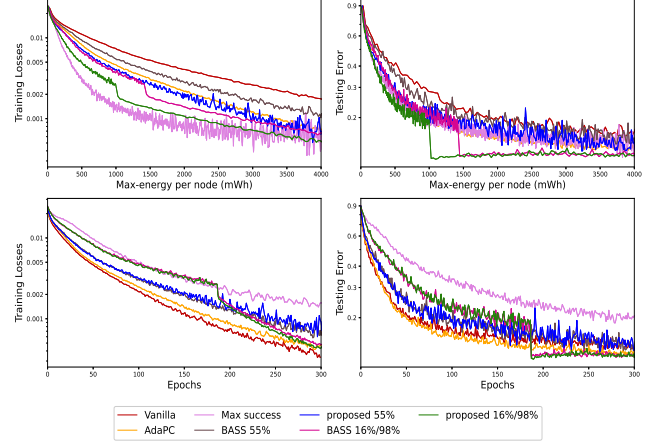


Fig. 3. Training performance on clique ('proposed/BASS $x\%$ ': 1-phase design activating $x\%$ of nodes; 'proposed/BASS $x\%/y\%$ ': 2-phase design activating $x\%$ of nodes in phase 1 and $y\%$ in phase 2).

the batch size to 64, the momentum to 0.9, and the weight decay to 0.0005. We employ two base topologies: (i) a 33-node clique, which represents a densely deployed wireless network where every node can reach every other node in one hop; (ii) the topology of Roofnet [56], which contains 33 nodes and 187 links. The data rate is set to 1 Mbps in both topologies according to [56].

2) *Cost Parameters:* We consider two types of devices commonly used for learning in edge networks: NVIDIA Tegra X2 (TX2) with Broadcom BCM4354 and Jetson Xavier NX with Intel 8265NGW, with a computation power of 4.7W/6.3W and a transmission power of 40mW/100mW, respectively [57]. Based on these parameters, we set the computation energy as $c_i^a = 0.086\text{mWh}$ for TX2 and 0.086mWh for NX, and the communication energy as $c_i^b = 0.533\text{mWh}$ for TX2 and 1.333mWh for NX⁴. We assign odd-numbered nodes to TX2 and even-numbered nodes to NX.

3) *Benchmarks:* We compare the proposed solution with the following benchmarks:

- 'Vanilla D-PSGD' [1], which is a baseline with all the neighbors communicating in all the iterations;

⁴Our model size is $S = 6\text{MB}$ at FP32, batch size is $B = 64$, and processing speed is $t_i^c = 1.026\text{ms}$ per sample for TX2 and 0.769ms per sample for NX. Under 1Mbps, we estimate the computation energy by $c_i^a = P_i^c * B * t_i^c / 3600 \text{ mWh}$, and the communication energy by $c_i^b = P_i^t * S * 8 / 1 / 3600 \text{ mWh}$ (P_i^c : computation power of node i in \mathbf{W} ; P_i^t : transmission power of node i in mW).

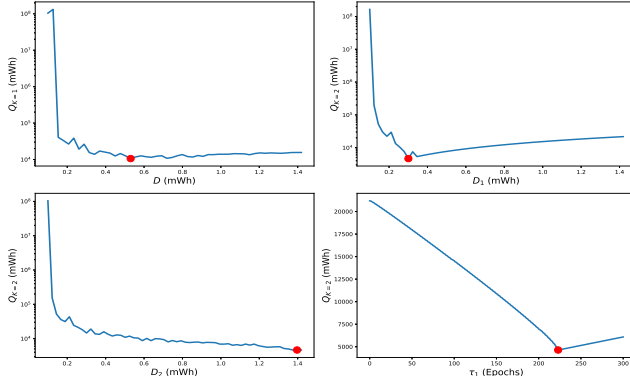


Fig. 4. Design objective vs. design parameters for Roofnet.

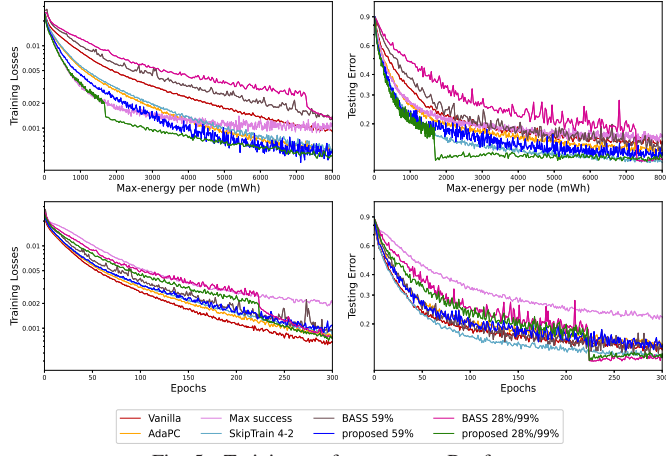


Fig. 5. Training performance on Roofnet.

- ‘AdaPC’ [45], where all the neighbors communicate periodically, with a period adapted according to [45, Alg. 2];
- ‘BASS’ [12], a state-of-the-art mixing matrix design for broadcast communication with a different objective of minimizing the communication time (by minimizing the number of collision-free transmission slots);
- ‘Max Success’ [29], another mixing matrix design for broadcast communication with a different objective of maximizing the expected number of successful links;
- ‘SkipTrain’ [28], which is the opposite of ‘AdaPC’ that periodically skips local updates⁵;

We note that under broadcast communication, the above benchmarks subsume the performance of several other existing solutions, e.g., [9] is subsumed by ‘BASS’ [12] and [7], [15] are subsumed by ‘Vanilla D-PSGD’.

B. Evaluation Results

1) *Results for Clique*: We first evaluate the design objective Q_K with respect to the budget D_s and the duration τ_s for each phase. Fig. 2 shows the results for $K = 1$ and $K = 2$, while fixing the other design parameters at their optimal values. The optimal value for each parameter is denoted by •. The results not only suggest the benefit of multi-phase design as the optimal value of $Q_{K=2}$ is smaller than the optimal

⁵For a fully connected base topology, ‘SkipTrain’ reduces to ‘Vanilla D-PSGD’, as there is no need for additional communications to achieve synchronization after a training round.

value of $Q_{K=1}$, but also indicate the need of switching from a lower level of activation to a higher level of activation (as $D_1 < D_2$). However, τ_s from this optimization is often larger than necessary as it is based on an upper bound on the total number of iterations. We thus normalize it by $\tau_s \cdot (T/\bar{T})$, where T is the actual number of iterations to reach convergence and \bar{T} is an upper bound.

We then evaluate the training performance in terms of training loss and testing error, omitting ‘SkipTrain’ as it reduces to ‘Vanilla’ in this case. As ‘BASS’ also has a configurable budget, we evaluate two versions of it with the same percentage of activated nodes as our 1-phase/2-phase designs. The results in Fig. 3 show that: (i) partial activation can achieve a better energy efficiency than activating all the nodes (‘Vanilla’); (ii) the proposed solution achieves a better tradeoff between the testing error and the maximum per-node energy consumption than the benchmarks, and 2-phase design outperforms 1-phase design.

2) *Results for Roofnet*: We repeat the experiments on Roofnet, where ‘SkipTrain’ is configured according to the recommendation by [28] for a topology of similar average degree. The results in Fig. 4–5 show similar observations as Fig. 2–3, except that (i) the design objective in Fig. 4 is based on numerically estimated ρ values as explained in Section V-B2 (from 500 matrices per budget), (ii) ‘BASS’ has a bigger performance gap with our solution due to its negligence of balancing energy consumption across nodes, and (iii) it takes more epochs and energy consumption to reach convergence due to the limited connectivity between nodes.

VIII. CONCLUSION

We considered the mixing matrix design to minimize the maximum per-node energy consumption in DFL while considering the broadcast nature of wireless communications. Based on a novel convergence theorem that allows arbitrarily time-varying mixing matrices, we proposed a multi-phase design framework that designs randomized mixing matrices as well as how long to use each matrix. Our evaluations on real data demonstrated that the proposed design can achieve a superior tradeoff between maximum per-node energy consumption and accuracy even with two phases, thus improving the energy efficiency of learning in wireless networks.

REFERENCES

- [1] X. Lian, C. Zhang, H. Zhang, C.-J. Hsieh, W. Zhang, and J. Liu, “Can decentralized algorithms outperform centralized algorithms? a case study for decentralized parallel stochastic gradient descent,” in *Proceedings of the 31st International Conference on Neural Information Processing Systems*, 2017, p. 5336–5346.
- [2] H. McMahan, E. Moore, D. Ramage, S. Hampson, and B. A. y Arcas, “Communication-efficient learning of deep networks from decentralized data,” in *AISTATS*, 2017.
- [3] P. Kairouz *et al.*, *Advances and Open Problems in Federated Learning*. Now Foundations and Trends, 2021.
- [4] L. Luo, P. West, J. Nelson, A. Krishnamurthy, and L. Ceze, “Plink: Discovering and exploiting locality for accelerated distributed training on the public cloud,” in *Proceedings of Machine Learning and Systems*, vol. 2, 2020, pp. 82–97.
- [5] X. Chen, G. Zhu, Y. Deng, and Y. Fang, “Federated learning over multi-hop wireless networks with in-network aggregation,” *IEEE Transactions on Wireless Communications*, vol. 21, no. 6, pp. 4622–4634, 2022.

[6] A. Koloskova, T. Lin, S. U. Stich, and M. Jaggi, “Decentralized deep learning with arbitrary communication compression,” in *The International Conference on Learning Representations (ICLR)*, 2020.

[7] C.-C. Chiu, X. Zhang, T. He, S. Wang, and A. Swami, “Laplacian matrix sampling for communication- efficient decentralized learning,” *IEEE Journal on Selected Areas in Communications*, vol. 41, no. 4, pp. 887–901, 2023.

[8] N. Singh, D. Data, J. George, and S. Diggavi, “SPARQ-SGD: Event-triggered and compressed communication in decentralized optimization,” in *IEEE CDC*, 2020.

[9] J. Wang, A. K. Sahu, G. Joshi, and S. Kar, “MATCHA: A matching-based link scheduling strategy to speed up distributed optimization,” *IEEE Transactions on Signal Processing*, vol. 70, pp. 5208–5221, 2022.

[10] Y. Hua, K. Miller, A. L. Bertozzi, C. Qian, and B. Wang, “Efficient and reliable overlay networks for decentralized federated learning,” *SIAM Journal on Applied Mathematics*, vol. 82, no. 4, pp. 1558–1586, 2022.

[11] B. Le Bars, A. Bellet, M. Tommasi, E. Lavoie, and A.-M. Kermarrec, “Refined convergence and topology learning for decentralized SGD with heterogeneous data,” in *International Conference on Artificial Intelligence and Statistics*. PMLR, 2023, pp. 1672–1702.

[12] D. P. Herrera, Z. Chen, and E. G. Larsson, “Faster convergence with less communication: Broadcast-based subgraph sampling for decentralized learning over wireless networks,” *IEEE Open Journal of the Communications Society*, pp. 1–1, 2025.

[13] H. Xing, O. Simeone, and S. Bi, “Federated learning over wireless device-to-device networks: Algorithms and convergence analysis,” *IEEE Journal on Selected Areas in Communications*, vol. 39, no. 12, pp. 3723–3741, 2021.

[14] P. Pinyoanuntapong, W. H. Huff, M. Lee, C. Chen, and P. Wang, “Toward scalable and robust AloT via decentralized federated learning,” *IEEE Internet of Things Magazine*, vol. 5, no. 1, pp. 30–35, 2022.

[15] X. Zhang, C.-C. Chiu, and T. He, “Energy-efficient decentralized learning via graph sparsification,” 2024, <https://arxiv.org/abs/2401.03083>.

[16] H. Tang, X. Lian, M. Yan, C. Zhang, and J. Liu, “ d^2 : Decentralized training over decentralized data,” in *Proceedings of the 35th International Conference on Machine Learning, ICML*, 2018.

[17] Y. Lu and C. D. Sa, “Optimal complexity in decentralized training,” in *International Conference on Machine Learning (ICML)*, 2021.

[18] R. Xin, U. Khan, and S. Kar, “A hybrid variance-reduced method for decentralized stochastic non-convex optimization,” in *Proceedings of the 38th International Conference on Machine Learning*, ser. Proceedings of Machine Learning Research, M. Meila and T. Zhang, Eds., vol. 139. PMLR, 18–24 Jul 2021, pp. 11459–11469. [Online]. Available: <https://proceedings.mlr.press/v139/xin21a.html>

[19] L. Li, L. Yang, X. Guo, Y. Shi, H. Wang, W. Chen, and K. B. Letaief, “Delay analysis of wireless federated learning based on saddle point approximation and large deviation theory,” *IEEE Journal on Selected Areas in Communications*, vol. 39, no. 12, pp. 3772–3789, 2021.

[20] Y. Lu and C. D. Sa, “Moniqua: Modulo quantized communication in decentralized SGD,” in *International Conference on Machine Learning (ICML)*, 2020.

[21] H. Tang, S. Gan, C. Zhang, T. Zhang, and J. Liu, “Communication compression for decentralized training,” in *Advances in Neural Information Processing Systems (NeurIPS)*, 2018.

[22] X. Zhang, J. Liu, Z. Zhu, and E. S. Bentley, “Communication-efficient network-distributed optimization with differential-coded compressors,” in *IEEE INFOCOM*, 2020, p. 317–326.

[23] J. Wang and G. Joshi, “Adaptive communication strategies to achieve the best error-runtime trade-off in local-update SGD,” in *Systems for ML*, 2019.

[24] N. H. Tran, W. Bao, A. Zomaya, M. N. Nguyen, and C. S. Hong, “Federated learning over wireless networks: Optimization model design and analysis,” in *IEEE INFOCOM*, 2019.

[25] S. Wang, T. Tuor, T. Salonidis, K. K. Leung, C. Makaya, T. He, and K. Chan, “Adaptive federated learning in resource constrained edge computing systems,” *IEEE Journal on Selected Areas in Communications*, vol. 37, no. 6, pp. 1205–1221, 2019.

[26] J. Wang and G. Joshi, “Cooperative sgd: A unified framework for the design and analysis of local-update sgd algorithms,” *Journal of Machine Learning Research*, vol. 22, no. 213, pp. 1–50, 2021. [Online]. Available: <http://jmlr.org/papers/v22/20-147.html>

[27] N. Singh, D. Data, J. George, and S. Diggavi, “SQuARM-SGD: Communication-efficient momentum SGD for decentralized optimization,” *IEEE Journal on Selected Areas in Information Theory*, vol. 2, no. 3, pp. 954–969, 2021.

[28] M. De Vos, A. Dhasade, P. Dini, E. Guerra, A.-M. Kermarrec, M. Miozzo, R. Pires, and R. Sharma, “Energy-aware decentralized learning with intermittent model training,” in *2024 IEEE International Parallel and Distributed Processing Symposium Workshops (IPDPSW)*, 2024, pp. 1172–1174.

[29] Z. Chen, M. Dahl, and E. G. Larsson, “Decentralized learning over wireless networks: The effect of broadcast with random access,” in *2023 IEEE 24th International Workshop on Signal Processing Advances in Wireless Communications (SPAWC)*, 2023, pp. 316–320.

[30] G. Neglia, C. Xu, D. Towsley, and G. Calbi, “Decentralized gradient methods: does topology matter?” in *International Conference on Artificial Intelligence and Statistics*. PMLR, 2020, pp. 2348–2358.

[31] Z. Jiang, Y. Xu, H. Xu, L. Wang, C. Qiao, and L. Huang, “Joint model pruning and topology construction for accelerating decentralized machine learning,” *IEEE Transactions on Parallel and Distributed Systems*, 2023.

[32] T. Vogels, H. Hendrikx, and M. Jaggi, “Beyond spectral gap: The role of the topology in decentralized learning,” *Advances in Neural Information Processing Systems*, vol. 35, pp. 15 039–15 050, 2022.

[33] W. Liu, L. Chen, and W. Zhang, “Decentralized federated learning: Balancing communication and computing costs,” *IEEE Transactions on Signal and Information Processing over Networks*, vol. 8, pp. 131–143, 2022.

[34] A. Koloskova, N. Loizou, S. Boreiri, M. Jaggi, and S. Stich, “A unified theory of decentralized SGD with changing topology and local updates,” in *ICML*, 2020.

[35] A. Nedić and A. Olshevsky, “Distributed optimization over time-varying directed graphs,” *IEEE Transactions on Automatic Control*, vol. 60, no. 3, pp. 601–615, 2015.

[36] A. Nedić, A. Olshevsky, and W. Shi, “Achieving geometric convergence for distributed optimization over time-varying graphs,” *SIAM Journal on Optimization*, vol. 27, no. 4, pp. 2597–2633, 2017. [Online]. Available: <https://doi.org/10.1137/16M1084316>

[37] H. Li and Z. Lin, “Accelerated gradient tracking over time-varying graphs for decentralized optimization,” *Journal of Machine Learning Research*, vol. 25, no. 274, pp. 1–52, 2024. [Online]. Available: <http://jmlr.org/papers/v25/21-0475.html>

[38] X. Huang and K. Yuan, “Optimal complexity in non-convex decentralized learning over time-varying networks,” 2022. [Online]. Available: <https://arxiv.org/abs/2211.00533>

[39] R. Hönig, Y. Zhao, and R. Mullins, “DAdaQuant: Doubly-adaptive quantization for communication-efficient federated learning,” in *Proceedings of the 39th International Conference on Machine Learning*, ser. Proceedings of Machine Learning Research, K. Chaudhuri, S. Jegelka, L. Song, C. Szepesvari, G. Niu, and S. Sabato, Eds., vol. 162. PMLR, 17–23 Jul 2022, pp. 8852–8866. [Online]. Available: <https://proceedings.mlr.press/v162/honig22a.html>

[40] Y. Zhuansun, D. Li, X. Huang, and C. Sun, “Communication-efficient federated learning with adaptive compression under dynamic bandwidth,” 2024. [Online]. Available: <https://arxiv.org/abs/2405.03248>

[41] L. Wang, X. Xu, and J. Pei, “Communication-efficient federated learning via dynamic sparsity: An adaptive pruning ratio based on weight importance,” *IEEE Transactions on Cognitive Communications and Networking*, pp. 1–1, 2025.

[42] Y. He, Y. Chen, X. Yang, Y. Zhang, and B. Zeng, “Class-wise adaptive self distillation for federated learning on non-iid data (student abstract),” *Proceedings of the AAAI Conference on Artificial Intelligence*, vol. 36, no. 11, pp. 12 967–12 968, Jun. 2022. [Online]. Available: <https://ojs.aaai.org/index.php/AAAI/article/view/21620>

[43] Y. Li, X. Wang, H. Li, P. K. Donta, M. Huang, and S. Dusdar, “Communication-efficient federated learning for heterogeneous clients,” *ACM Trans. Internet Technol.*, vol. 25, no. 2, Apr. 2025. [Online]. Available: <https://doi.org/10.1145/3716870>

[44] C. Chen, H. Xu, W. Wang, B. Li, B. Li, L. Chen, and G. Zhang, “Communication-Efficient Federated Learning with Adaptive Parameter Freezing,” in *2021 IEEE 41st International Conference on Distributed Computing Systems (ICDCS)*. Los Alamitos, CA, USA: IEEE Computer Society, Jul. 2021, pp. 1–11. [Online]. Available: <https://doi.ieeecomputersociety.org/10.1109/ICDCS51616.2021.00010>

[45] J. Tchaye-Kondi, Y. Zhai, J. Shen, A. Telikani, and L. Zhu, “Adaptive period control for communication efficient and fast convergent federated learning,” *IEEE Transactions on Mobile Computing*, vol. 23, no. 12, pp. 12 572–12 586, 2024.

[46] H. Zhang, Z. Xie, R. Zarei, T. Wu, and K. Chen, “Adaptive client selection in resource constrained federated learning systems: A deep

reinforcement learning approach,” *IEEE Access*, vol. 9, pp. 98423–98432, 2021.

[47] H. Xu, M. Chen, Z. Meng, Y. Xu, L. Wang, and C. Qiao, “Decentralized machine learning through experience-driven method in edge networks,” *IEEE Journal on Selected Areas in Communications*, vol. 40, no. 2, pp. 515–531, 2022.

[48] Y. Liao, Y. Xu, H. Xu, L. Wang, C. Qian, and C. Qiao, “Decentralized federated learning with adaptive configuration for heterogeneous participants,” *IEEE Transactions on Mobile Computing*, vol. 23, no. 6, p. 7453–7469, Jun. 2024. [Online]. Available: <https://doi.org/10.1109/TMC.2023.3335403>

[49] C. Blair, “Problem complexity and method efficiency in optimization (a. s. nemirovsky and d. b. yudin),” *SIAM Review*, vol. 27, no. 2, pp. 264–265, 1985. [Online]. Available: <https://doi.org/10.1137/1027074>

[50] L. Xiao, S. P. Boyd, and S. Lall, “Distributed average consensus with time-varying metropolis weights,” 2006, unpublished manuscript. [Online]. Available: <https://api.semanticscholar.org/CorpusID:123313438>

[51] Y. Wang, L. Lin, and J. Chen, “Communication-efficient adaptive federated learning,” in *Proceedings of the 39th International Conference on Machine Learning*, ser. Proceedings of Machine Learning Research, K. Chaudhuri, S. Jegelka, L. Song, C. Szepesvari, G. Niu, and S. Sabato, Eds., vol. 162. PMLR 17–23 Jul 2022, pp. 22 802–22 838. [Online]. Available: <https://proceedings.mlr.press/v162/wang22o.html>

[52] G. Nadiradze, A. Sabour, P. Davies, S. Li, and D. Alistarh, “Asynchronous decentralized sgd with quantized and local updates,” in *Proceedings of the 35th International Conference on Neural Information Processing Systems*, ser. NIPS ’21. Red Hook, NY, USA: Curran Associates Inc., 2021.

[53] P. Zhou, Q. Lin, D. Loghin, B. C. Ooi, Y. Wu, and H. Yu, “Communication-efficient decentralized machine learning over heterogeneous networks,” in *2021 IEEE 37th International Conference on Data Engineering (ICDE)*, 2021, pp. 384–395.

[54] J. Wang, A. K. Sahu, G. Joshi, and S. Kar, “Exploring the error-runtime trade-off in decentralized optimization,” in *2020 54th Asilomar Conference on Signals, Systems, and Computers*, 2020, pp. 910–914.

[55] S. Hoory, N. Linial, and A. Wigderson, “Expander graphs and their applications,” *Bull. Amer. Math. Soc.*, vol. 43, no. 04, p. 439–562, Aug. 2006.

[56] D. Aguayo, J. Bicket, S. Biswas, G. Judd, and R. Morris, “Link-level measurements from an 802.11b mesh network,” in *SIGCOMM*, 2004.

[57] X. Qiu, T. Parcollet, J. Fernandez-Marques, P. P. B. Gusmao, D. J. Beutel, T. Topal, A. Mathur, and N. D. Lane, “A first look into the carbon footprint of federated learning,” 2021. [Online]. Available: <https://arxiv.org/abs/2102.07627>

[58] K. Yuan, Q. Ling, and W. Yin, “On the convergence of decentralized gradient descent,” *SIAM Journal on Optimization*, vol. 26, no. 3, pp. 1835–1854, 2016. [Online]. Available: <https://doi.org/10.1137/130943170>

APPENDIX

A. Proof of Theorem III.2

We use the following notation for the “consensus distance” at iteration t :

$$\Xi_t := \frac{1}{m} \mathbf{E} \sum_{i=1}^m \|x_i^{(t)} - \bar{x}^{(0)}\|^2.$$

We use $\mathbf{E}_{t+1}[\cdot]$ to denote the conditional expectation $\mathbf{E}[\cdot \mid \{x_i^{(t)}\}]$. Also, we let x^* denote the optimal parameter vector of $F(\cdot)$ and let $F_{\inf} := F(x^*)$.

Lemma A.1 (Lemma 11, [34]). Under assumptions (1)-(3), D-PSGD with stepsize $\eta < \frac{1}{4L(M_1+1)}$ satisfies

$$\mathbf{E}_{t+1}[F(\bar{x}^{(t+1)})] \leq F(\bar{x}^{(t)}) - \frac{\eta}{4} \|\nabla F(\bar{x}^{(t)})\|_2^2 + \eta L^2 \Xi_t + \frac{\eta^2 L \hat{\sigma}^2}{m} \Xi_t \leq \nu_0^t \Xi_0 + 2\eta^2 \sum_{j=0}^{t-1} \nu_{j+1}^t \left[\left(\frac{6}{p^{(j)}} + M_1 \right) (M_2 e_j + \hat{\zeta}^2) + \hat{\sigma}^2 \right].$$

Lemma A.2. Under assumptions (1)-(3), D-PSGD with the stepsize $\eta \leq \frac{p^{(t-1)}}{8L\sqrt{12+2p^{(t-1)}M_1}}$ satisfies

$$\Xi_t \leq \left(1 - \frac{p^{(t-1)}}{2}\right) \Xi_{t-1} + 2\eta^2 \left[\left(\frac{6}{p^{(t-1)}} + M_1 \right) (M_2 \|\nabla F(\bar{x}^{(t-1)})\|^2 + \hat{\zeta}^2) + \hat{\sigma}^2 \right].$$

Noting that the parameter $p^{(t-1)}$ in [34] is originally defined in a different form, but due to Lemma 3.1 in [15], it can be treated the same, in the case of $\tau = 1$. Then Lemma A.2 follows from Lemma 12 in [34] by setting $\tau = 1$ and improving some constants in this special case.

Proof of Theorem III.2. We define the following notations for ease of the proof:

- $f_t := \mathbf{E}[F(\bar{x}^{(t)})] - F_{\inf}$.
- $e_t := \mathbf{E}\|\nabla F(\bar{x}^{(t)})\|^2$.
- $\nu_j^t := \prod_{i=j}^{t-1} \left(1 - \frac{p_i}{2}\right)$.
- $\kappa := \frac{\sqrt{(1+M_1)(1+M_2)}}{p_{\min}}$.
- $\Upsilon := M_2 \max_j \left(\frac{6\pi_j}{p^{(j)}} + M_1 \pi_j \right)$.

In these notations, Lemma A.1 implies

$$f_{t+1} \leq f_t - \frac{\eta}{4} e_t + \frac{L\hat{\sigma}^2\eta^2}{m} + \eta L^2 \Xi_t, \quad (25)$$

and Lemma A.2 upper bounds Ξ_t by

$$\Xi_t \leq \left(1 - \frac{p^{(t-1)}}{2}\right) \Xi_{t-1} + 2\eta^2 \left[\left(\frac{6}{p^{(t-1)}} + M_1 \right) (M_2 e_{t-1} + \hat{\zeta}^2) + \hat{\sigma}^2 \right]. \quad (26)$$

We un-roll the recursion in (26) to obtain

Noting that $\pi_j = \sum_{t>j} \nu_{j+1}^t$, we sum over t up to T and get

$$\begin{aligned}
\sum_{t=1}^T \Xi_t &\leq \sum_{t=1}^T \nu_0^t \Xi_0 + 2\eta^2 \sum_{t=1}^T \sum_{j=0}^{t-1} \nu_{j+1}^t \\
&\quad \left[\left(\frac{6}{p^{(j)}} + M_1 \right) (M_2 e_j + \hat{\zeta}^2) + \hat{\sigma}^2 \right] \\
&\leq \sum_{t=1}^T \nu_0^t \Xi_0 + 12\eta^2 \hat{\zeta}^2 \sum_{j=0}^{T-1} \sum_{t=j+1}^T \frac{\nu_{j+1}^t}{p^{(j)}} \\
&\quad + 2\eta^2 (\hat{\sigma}^2 + M_1 \hat{\zeta}^2) \sum_{j=0}^{T-1} \sum_{t=j+1}^T \nu_{j+1}^t \\
&\quad + 2\eta^2 \sum_{j=0}^{T-1} M_2 \left(\frac{6}{p^{(j)}} + M_1 \right) e_j \sum_{t=j+1}^T \nu_{j+1}^t \\
&\leq (1 + \pi_0) \Xi_0 + 12\eta^2 \hat{\zeta}^2 \sum_{j=0}^{T-1} \frac{\pi_j}{p_j} \\
&\quad + 2\eta^2 \sum_{j=0}^{T-1} (\hat{\sigma}^2 + M_1 \hat{\zeta}^2) \pi_j \\
&\quad + 2\eta^2 \sum_{j=0}^{T-1} M_2 \left(\frac{6}{p^{(j)}} + M_1 \right) e_j \pi_j \\
&\leq (1 + \pi_0) \Xi_0 + 2\eta^2 \Upsilon \sum_{j=0}^{T-1} e_j \\
&\quad + 2\eta^2 T [(\hat{\sigma}^2 + M_1 \hat{\zeta}^2) \Pi_1(T) + 6\hat{\zeta}^2 \Pi_2(T)].
\end{aligned}$$

Next we move f_t in (25) to the right-hand side and average it over time to get

$$\frac{1}{8T} \sum_{t=0}^{T-1} e_t \leq \frac{1}{T} \sum_{t=0}^{T-1} \frac{f_t - f_{t+1}}{\eta} + \frac{\eta L \hat{\sigma}^2}{m} + \frac{L^2}{T} \sum_{t=0}^{T-1} \Xi_t. \quad (27)$$

Now we plug in the bound for $\sum_{t=1}^T \Xi_t$ to (27) and obtain

$$\sum_{t=0}^{T-1} \frac{e_t}{8T} \leq \frac{f_0}{T\eta} + \frac{\eta L \hat{\sigma}^2}{m} + \frac{L^2(2 + \pi_0) \Xi_0}{T} + \frac{2L^2 \eta^2 \Upsilon}{T} \sum_{j=0}^{T-1} e_j \quad (28)$$

$$+ 2\eta^2 L^2 [(\hat{\sigma}^2 + M_1 \hat{\zeta}^2) \Pi_1(T) + 6\hat{\zeta}^2 \Pi_2(T)]. \quad (29)$$

We let $\alpha(T) := 2L^2 [(\hat{\sigma}^2 + M_1 \hat{\zeta}^2) \Pi_1(T) + 6\hat{\zeta}^2 \Pi_2(T)]$. We need the learning rate to satisfy the conditions in Lemmas A.1–A.2. By choosing a sufficiently small learning rate⁶

$$\eta = \min \left\{ \left(\frac{mf_0}{\hat{\sigma}^2 LT} \right)^{\frac{1}{2}}, \left(\frac{f_0}{T\alpha(T)} \right)^{\frac{1}{3}}, \frac{1}{20L\kappa}, \frac{1}{4L(M_1 + 1)} \right\},$$

⁶While the choice of η in [34] does not explicitly include the term $(4L(M_1 + 1))^{-1}$, we believe that, without this additional term, the condition required by Lemma A.1 may not hold in general.

the learning rate satisfies the conditions in Lemma A.1 and A.2. Moreover, we claim that $\eta^2 \leq \frac{1}{32L^2\Upsilon}$. Indeed,

$$\begin{aligned}
\eta^2 &\leq \frac{1}{400L^2\kappa^2} \leq \min_j \frac{(p^{(j)})^2}{32L^2(M_2 + 1)(12 + 2M_1 p^{(j)})} \\
&\leq \frac{1}{32L^2 \max_j \left\{ \frac{2M_1 M_2}{p^{(j)}} + \frac{12M_2}{(p^{(j)})^2} \right\}}
\end{aligned}$$

Let j^* denote the index of j that maximizes $\max_j \left(\frac{6\pi_j}{p^{(j)}} + M_1 \pi_j \right)$, that is, the index of j which yields Υ . By Lemma III.1, $\pi_{j^*} \leq \max_j \frac{2}{p^{(j)}}$, so

$$\begin{aligned}
\max_j \left\{ \frac{2M_1 M_2}{p^{(j)}} + \frac{12M_2}{(p^{(j)})^2} \right\} &\geq M_1 M_2 \pi_{j^*} + \max_j \frac{6M_2 \pi_{j^*}}{p^{(j)}} \\
&\geq M_1 M_2 \pi_{j^*} + \frac{6M_2 \pi_{j^*}}{p^{(j^*)}} = \Upsilon.
\end{aligned}$$

Then it follows that $\eta^2 \leq \frac{1}{32L^2\Upsilon}$ and

$$\frac{2L^2 \eta^2 \Upsilon}{T} \sum_{j=0}^{T-1} e_j \leq \sum_{j=0}^{T-1} \frac{e_j}{16}. \quad (30)$$

In addition, since $\eta \leq \min \left\{ \left(\frac{mf_0}{\hat{\sigma}^2 LT} \right)^{\frac{1}{2}}, \left(\frac{f_0}{T\alpha(T)} \right)^{\frac{1}{3}} \right\}$, we obtain

$$\frac{\eta L \hat{\sigma}^2}{m} \leq \left(\frac{\hat{\sigma}^2 L f_0}{m T} \right)^{\frac{1}{2}} \quad (31)$$

and

$$\eta^2 \alpha(T) \leq \left(\frac{f_0^2 \alpha(T)}{T^2} \right)^{\frac{1}{3}} \quad (32)$$

respectively. Finally,

$$\frac{f_0}{T\eta} = \frac{f_0}{T} \cdot \max \left\{ \left(\frac{\hat{\sigma}^2 L T}{m f_0} \right)^{\frac{1}{2}}, \left(\frac{T \alpha(T)}{f_0} \right)^{\frac{1}{3}}, 20L\kappa, 4L(M_1 + 1) \right\} \quad (33)$$

$$= \max \left\{ \left(\frac{\hat{\sigma}^2 L f_0}{m T} \right)^{\frac{1}{2}}, \left(\frac{f_0^2 \alpha(T)}{T^2} \right)^{\frac{1}{3}}, \frac{20L\kappa f_0}{T}, \frac{4f_0 L(M_1 + 1)}{T} \right\}. \quad (34)$$

Combining inequalities (28)–(34) implies that

$$\begin{aligned}
\sum_{t=0}^{T-1} \frac{e_t}{16T} &\leq 2 \left(\frac{\hat{\sigma}^2 L f_0}{m T} \right)^{\frac{1}{2}} + 2 \left(\frac{f_0^2 \alpha(T)}{T^2} \right)^{\frac{1}{3}} + \frac{L^2(2 + \pi_0) \Xi_0}{T} \\
&\quad + \frac{20L\kappa f_0}{T} + \frac{4f_0 L(M_1 + 1)}{T}.
\end{aligned}$$

The theorem follows by setting the right-hand side to be at most $\epsilon/16$. \square

B. Convergence Theorem for Convex Objectives

The convergence of D-PSGD for convex objectives is established under the following assumptions:

(4) Each local objective function $F_i(\mathbf{x})$ is L -Lipschitz smooth and convex, i.e., for $x, x' \in \mathbb{R}^d$,

$$F_i(x) - F_i(x') \leq \langle \nabla F_i(x), x - x' \rangle.$$

(5) There exist a constant $\hat{\sigma} > 0$ such that

$$\frac{1}{m} \sum_{i \in V} \mathbf{E}[\|g(\mathbf{x}^*; \xi_i) - \nabla F_i(\mathbf{x}^*)\|^2] \leq \hat{\sigma}^2.$$

(6) There exist a constant $\hat{\zeta} > 0$ such that

$$\frac{1}{m} \sum_{i \in V} \|\nabla F_i(\mathbf{x}^*)\|^2 \leq \hat{\zeta}^2.$$

While condition (4) is stronger than condition (1), the additional convexity assumption allows conditions (5)–(6) to be significantly weaker than conditions (2)–(3): not only can we set $M_1 = M_2 = 0$, but it also suffices to impose the two noise bounds only at $x = x^*$.

Theorem A.3. The D-PSGD under assumptions (4)–(6) can achieve ϵ -convergence (i.e., $\frac{1}{T} \sum_{t=0}^{T-1} (\mathbf{E}[F(\bar{\mathbf{x}}^{(t)})] - F_{\inf}) \leq \epsilon$) when the number of iterations T satisfies $T \geq T_4(\Pi_1(T), \Pi_2(T), \pi_0, p_{\min}, \epsilon, \bar{\mathbf{x}}^{(0)})$ for

$$T_4(\Pi_1, \Pi_2, \pi_0, p_{\min}, \epsilon, \bar{\mathbf{x}}^{(0)}) := r_0. \quad (35)$$

$$O \left(\frac{\hat{\sigma}^2}{m\epsilon^2} + \frac{\sqrt{(\hat{\sigma}^2\Pi_1 + \hat{\zeta}^2\Pi_2)L}}{\epsilon^{3/2}} + \frac{(1 + \pi_0)L\Xi_0}{\epsilon} + \frac{L}{\epsilon p_{\min}} \right), \quad (36)$$

where $r_0 := \|\bar{\mathbf{x}}^{(0)} - \mathbf{x}^*\|^2$ (\mathbf{x}^* denotes the optimal parameter vector) and $\Xi_0 := \frac{1}{m} \sum_{i=1}^m \|x_i^{(0)} - \bar{\mathbf{x}}^{(0)}\|^2$.

Convergence analyses of gossip-based algorithms on static communication graphs, such as Decentralized Gradient Descent (DGD) [58], are well established. For time-varying topologies, D-PSGD [34] establishes convergence under periodic communication patterns, while gradient-tracking variants have been analyzed in [35] and [36] under stronger assumptions. Our approach is most closely related to [34], but it removes the periodicity assumption and applies to arbitrary time-varying graphs.

Lemma A.4 (Lemma 8, [34]). Under assumptions (4)–(6), D-PSGD with the stepsize $\eta \leq \frac{1}{12L}$ satisfies

$$\begin{aligned} \mathbf{E}_{t+1}[\|\bar{\mathbf{x}}^{(t+1)} - \mathbf{x}^*\|^2] &\leq \|\bar{\mathbf{x}}^{(t)} - \mathbf{x}^*\|^2 \\ &\quad - \eta(F(\bar{\mathbf{x}}^{(t)}) - F^*) + \frac{\hat{\sigma}^2\eta^2}{m} + 3\eta L\Xi_t, \end{aligned}$$

when local functions F_i 's are convex.

Lemma A.5. Under assumptions (4)–(6), D-PSGD with the stepsize $\eta \leq \frac{p^{(t-1)}}{400L}$ satisfies

$$\begin{aligned} \Xi_t &\leq \left(1 - \frac{p^{(t-1)}}{2}\right)\Xi_{t-1} + \eta^2 \cdot \\ &\quad \left[\frac{72L}{p^{(t-1)}} \mathbf{E}(F(\bar{\mathbf{x}}^{(t-1)}) - F_{\inf}) + 8\hat{\sigma}^2 + \frac{18\hat{\zeta}^2}{p^{(t-1)}} \right], \end{aligned}$$

when local functions F_i 's are convex.

Analogous to Lemma A.2, Lemma A.5 follows directly from Lemma 3.1 in [15] and Lemma 8 in [34] by setting $\tau = 1$ and appropriately adjusting the constants.

Proof of Theorem A.3. We introduce several notations to simplify the expressions:

- $r_t := \mathbf{E}[\|\bar{\mathbf{x}}^{(t)} - \mathbf{x}^*\|^2]$.

- $f_t := \mathbf{E}F(\bar{\mathbf{x}}^{(t)}) - F^*$.
- $\Upsilon := \sqrt{\max_j(\pi_j/p^{(j)})}$.

To control the error at each t , we first apply the standard 1-step descent contraction by Lemma A.4 and obtain

$$r_{t+1} \leq r_t - \eta f_t + \frac{\hat{\sigma}^2\eta^2}{m} + 3\eta L\Xi_t. \quad (37)$$

Next we apply the upper bound on the consensus distance by Lemma A.5 for every $t \geq 1$:

$$\Xi_t \leq \left(1 - \frac{p^{(t-1)}}{2}\right)\Xi_{t-1} + \eta^2 \left[\frac{72Lf_{t-1}}{p^{(t-1)}} + 8\hat{\sigma}^2 + \frac{18\hat{\zeta}^2}{p^{(t-1)}} \right]. \quad (38)$$

We un-roll the recursion in (38) to obtain

$$\begin{aligned} \Xi_t &\leq \left[\prod_{j=0}^{t-1} \left(1 - \frac{p^{(j)}}{2}\right) \right] \Xi_0 + 72\eta^2 L \sum_{j=0}^{t-1} \left[\frac{f_j}{p^{(j)}} \prod_{i=j+1}^{t-1} \left(1 - \frac{p^{(i)}}{2}\right) \right] \\ &\quad + \eta^2 \sum_{j=1}^{t-1} \left[\left(8\hat{\sigma}^2 + \frac{18\hat{\zeta}^2}{p^{(j)}}\right) \cdot \prod_{i=j+1}^{t-1} \left(1 - \frac{p^{(i)}}{2}\right) \right]. \end{aligned}$$

We sum up Ξ_t for $t = 1, \dots, T$.

$$\begin{aligned} \sum_{t=1}^T \Xi_t &\leq \left[\sum_{t=1}^T \prod_{j=0}^{t-1} \left(1 - \frac{p^{(j)}}{2}\right) \right] \Xi_0 \\ &\quad + 72\eta^2 L \sum_{t=1}^T \sum_{j=0}^{t-1} \left[\frac{f_j}{p^{(j)}} \prod_{i=j+1}^{t-1} \left(1 - \frac{p^{(i)}}{2}\right) \right] \\ &\quad + 18\eta^2 \sum_{t=1}^T \sum_{j=0}^{t-1} \left[\left(\hat{\sigma}^2 + \frac{\hat{\zeta}^2}{p^{(j)}}\right) \prod_{i=j+1}^{t-1} \left(1 - \frac{p^{(i)}}{2}\right) \right] \\ &\leq \left[\sum_{t=1}^T \prod_{j=1}^{t-1} \left(1 - \frac{p^{(j)}}{2}\right) \right] \Xi_0 \\ &\quad + 72\eta^2 L \left[\sum_{j=0}^{T-1} \frac{f_j}{p^{(j)}} \left(\sum_{T \geq t > j} \prod_{i=j+1}^{t-1} \left(1 - \frac{p^{(i)}}{2}\right) \right) \right] \\ &\quad + 18\eta^2 \sum_{j=0}^{T-1} \left[\left(\hat{\sigma}^2 + \frac{\hat{\zeta}^2}{p^{(j)}}\right) \sum_{T \geq t > j} \prod_{i=j+1}^{t-1} \left(1 - \frac{p^{(i)}}{2}\right) \right] \\ &\leq \pi_0 \Xi_0 + 72\eta^2 L \sum_{j=0}^{T-1} \frac{f_j \pi_j}{p^{(j)}} + 18\eta^2 \sum_{j=0}^{T-1} \left(\hat{\sigma}^2 + \frac{\hat{\zeta}^2}{p^{(j)}}\right) \pi_j. \end{aligned}$$

We average (37) over t followed by plugging in the inequality

above to obtain

$$\begin{aligned}
\frac{1}{T} \sum_{t=0}^{T-1} f_t &\leq \frac{1}{T} \sum_{t=0}^{T-1} \frac{r_t - r_{t+1}}{\eta} + \frac{\eta \hat{\sigma}^2}{m} + \frac{3L}{T} \sum_{t=0}^{T-1} \Xi_t \\
&\leq \frac{r_0}{T\eta} + \frac{\eta \hat{\sigma}^2}{m} + \frac{3L}{T} \\
&\left((1 + \pi_0) \Xi_0 + 72\eta^2 L \sum_{j=0}^{T-2} \frac{f_j \pi_j}{p^{(j)}} + 18\eta^2 \sum_{j=0}^{T-2} (\hat{\sigma}^2 + \frac{\hat{\zeta}^2}{p^{(j)}}) \pi_j \right) \\
&\leq \frac{r_0}{T\eta} + \frac{\eta \hat{\sigma}^2}{m} + \frac{3L(1 + \pi_0) \Xi_0}{T} + \frac{216L^2 \eta^2 \Upsilon^2}{T} \sum_{j=0}^{T-2} f_j \\
&+ 54L\eta^2 (\hat{\sigma}^2 \Pi_1(T) + \hat{\zeta}^2 \Pi_2(T)).
\end{aligned}$$

We choose the learning rate to be

$$\eta := \min \left\{ \left(\frac{mr_0}{\hat{\sigma}^2 T} \right)^{\frac{1}{2}}, \min_t \frac{p^{(t)}}{900L}, \left(\frac{r_0}{T L(\Pi_1(T) \hat{\sigma}^2 + \hat{\zeta}^2 \Pi_2(T))} \right)^{\frac{1}{3}} \right\}.$$

It is straightforward to see that with the current choice $\eta < \frac{1}{12L}$. Thus, η satisfies conditions of both Lemma A.4 and A.5. Also, observe that by Lemma III.1 $\pi_t \leq \frac{2}{\min_j p^{(j)}}$ for all $t \geq 0$. Let j^* denote the index that maximizes $\pi_j / p^{(j)}$. It follows that

$$\max_j \frac{2}{(p^{(j)})^2} \geq \frac{1}{p^{(j^*)}} \cdot \frac{2}{\min_j p^{(j)}} \geq \frac{\pi_{j^*}}{p^{(j^*)}},$$

so we have $\eta^2 \leq (450L^2 \Upsilon^2)^{-1}$ since $\eta < \min_t \frac{p^{(t)}}{900L}$.

Now we evaluate our upper bound for this choice of η . As $\eta^2 \leq (450L^2 \Upsilon^2)^{-1}$, we always get

$$\frac{216L^2 \eta^2 \Upsilon^2}{T} \sum_{j=0}^{T-2} f_j \leq \frac{1}{2T} \sum_{j=0}^{T-1} f_j.$$

Also, since $\eta \leq \left(\frac{r_0}{T L(\Pi_1(T) \hat{\sigma}^2 + \hat{\zeta}^2 \Pi_2(T))} \right)^{\frac{1}{3}}$, and $\eta^2 \leq \frac{mr_0}{\hat{\sigma}^2 T}$, we have

$$L\eta^2 (\hat{\sigma}^2 \Pi_1(T) + \hat{\zeta}^2 \Pi_2(T)) \leq \frac{r_0^{2/3}}{T^{2/3}} (L(\Pi_1(T) \hat{\sigma}^2 + \Pi_2(T) \hat{\zeta}^2))^{1/3} \text{ for any } T \geq 1.$$

$$\text{and } \frac{\eta \hat{\sigma}^2}{m} \leq \sqrt{\frac{\hat{\sigma}^2 r_0}{m T}}.$$

Finally, when $\eta = \left(\frac{mr_0}{\hat{\sigma}^2 T} \right)^{\frac{1}{2}}$, we have

$$\frac{r_0}{T\eta} = \sqrt{\frac{\hat{\sigma}^2 r_0}{m T}}.$$

When $\eta = \min_t \frac{p^{(t)}}{900L}$, we obtain

$$\frac{r_0}{T\eta} = \frac{900r_0L}{T \min_t p^{(t)}},$$

and when $\eta = \left(\frac{r_0}{T L(\Pi_1(T) \hat{\sigma}^2 + \hat{\zeta}^2 \Pi_2(T))} \right)^{\frac{1}{3}}$ we have

$$\frac{r_0}{T\eta} \leq \frac{r_0^{2/3}}{T^{2/3}} (L(\Pi_1(T) \hat{\sigma}^2 + \Pi_2(T) \hat{\zeta}^2))^{1/3}.$$

Therefore,

$$\begin{aligned}
\frac{1}{T} \sum_{t=0}^{T-1} f_t &\leq 4 \sqrt{\frac{\hat{\sigma}^2 r_0}{m T}} + \frac{6L(1 + \pi_0) \Xi_0}{T} + \frac{1800r_0L}{T \min_t p^{(t)}} \\
&+ \frac{220r_0^{2/3}}{T^{2/3}} (L(\Pi_1(T) \hat{\sigma}^2 + \Pi_2(T) \hat{\zeta}^2))^{1/3},
\end{aligned}$$

and the right-hand side can be upper bounded by ϵ when $T \geq T_4(\Pi_1(T), \Pi_2(T), \pi_0, p_{\min}, \epsilon, \bar{x}^{(0)})$. \square

C. Deferred Proofs

We now present proofs for Lemma III.1, Lemma IV.1, Lemma IV.2, and Theorem V.2.

Proof of Lemma III.1. By the definition of π_j and our assumption, we have:

$$\pi_j \leq \sum_{i>j} \prod_{t=j+1}^{i-1} \left(1 - \frac{\delta}{2}\right) \leq \sum_{t=0}^{\infty} \left(1 - \frac{\delta}{2}\right)^t = \frac{1}{1 - (1 - \frac{\delta}{2})} = \frac{2}{\delta}.$$

We have shown Item 1, and Item 2 follows from the definitions of $\Pi_1(T)$ and $\Pi_2(T)$. For Item 3, in the special case of $p^{(t)} \equiv p$, we have

$$\pi_0 = \pi_1 = \pi_2 = \dots = \sum_{t=0}^{\infty} \prod_{j=1}^t \left(1 - \frac{p^{(j)}}{2}\right).$$

Thus,

$$\Pi_1(T) = \pi_0 = \sum_{t=0}^{\infty} \prod_{j=1}^t \left(1 - \frac{p^{(j)}}{2}\right) = \sum_{t=0}^{\infty} \left(1 - \frac{p}{2}\right)^t = \frac{2}{p}, \quad (39)$$

and

$$\Pi_2(T) = \frac{\pi_0}{p} = \frac{2}{p^2}, \quad (40)$$

Proof of Lemma IV.1. For any fixed $i \in V$, by Hoeffding's concentration inequality, we have for any $y > 0$,

$$\Pr \left[\sum_{t=1}^T c_i(\mathbf{W}^{(t)}) \geq TD + y \right] \leq \exp \left(-\frac{2y^2}{TD^2} \right).$$

It follows a union bound that

$$\Pr \left[\max_i \sum_{t=1}^T c_i(\mathbf{W}^{(t)}) \geq TD + y \right] \leq m \cdot \exp \left(-\frac{2y^2}{TD^2} \right),$$

and by integration over y , we obtain that

$$\mathbf{E} \left[\max_i \sum_{t=1}^T c_i(\mathbf{W}^{(t)}) \right] \leq D \cdot \left(T + m \sqrt{\frac{T\pi}{8}} \right) =: q(T, D),$$

which complete the proof. \square

Proof of Lemma IV.2. If $j \geq \tau_1$, then Lemma III.1 implies that $\pi_j = \frac{2}{p_2}$ since $(p^{(t+\tau_1)})_{t \geq 0}$ can be treated as a constant sequence where $p^{t+\tau_1} \equiv p_2$. If $j < \tau_1$ then

$$\begin{aligned}\pi_j &= \sum_{i>j}^{\infty} \prod_{t=j+1}^{i-1} \left(1 - \frac{p^{(t)}}{2}\right) \\ &= \sum_{i>j}^{\tau_1} \prod_{t=j+1}^{i-1} \left(1 - \frac{p_1}{2}\right) + \left(1 - \frac{p_1}{2}\right)^{\tau_1-j} \sum_{i>\tau_1}^{\infty} \prod_{t=\tau_1+1}^{i-1} \left(1 - \frac{p_2}{2}\right) \\ &= \sum_{t=0}^{\tau_1-j} \left(1 - \frac{p_1}{2}\right)^t + \left(1 - \frac{p_1}{2}\right)^{\tau_1-j} \cdot \pi_{\tau_1} \\ &= \frac{2[1 - (1 - \frac{p_1}{2})^{\tau_1-j}]}{p_1} + \frac{2(1 - \frac{p_1}{2})^{\tau_1-j}}{p_2} \\ &= \frac{2}{p_1} - \left(1 - \frac{p_1}{2}\right)^{\tau_1-j} \left(\frac{2}{p_1} - \frac{2}{p_2}\right).\end{aligned}$$

Plugging the above into the definitions (6) yields the desired results. \square

Proof of Lemma V.1. We verify that the mixing matrix \mathbf{W} satisfies all the constraints in (20a)-(20d):

- Since we generate \mathbf{W} from a randomized procedure, $\sum_{\mathbf{W}} \Pr[\mathbf{W}] = 1$ is clearly satisfied.
- Symmetry of \mathbf{W} also follows from the construction.
- The constraints on row sum and column sum also follows from the construction.
- Since off-diagonal entries are only assigned non-zero weights in Line 14, the construction respects the topology constraint and thus \mathbf{W} satisfies (20d).
- For (20c), let $i \in V$ be any node such that $c_i^a + c_i^b > D$ (otherwise (20c) holds trivially). Observe that due to the aforementioned reason,

$$\Pr[\exists j \neq i : \mathbf{W}[i, j] \neq 0] \leq \Pr[i \in U],$$

and the latter probability is set to be at most $\frac{D-c_i^a}{c_i^b}$ in the step 1. Hence,

$$c_i^a + \Pr[\exists j \neq i : \mathbf{W}[i, j] \neq 0] c_i^b \leq c_i^a + \frac{(D-c_i^a)}{c_i^b} c_i^b = D.$$

Therefore, \mathbf{W} is a feasible solution to (20). \square

Proof of Theorem V.2. Notice if the base topology is a clique, then $V_i \equiv V$ for every $i \in V$. Hence, if $i \in U$, Algorithm 2 assigns $\mathbf{W}[i, j] = 1/|U|$ for all $j \in U$ in Lines 14-15. For

any $i, j \in V$ such that $i \neq j$, we have

$$\begin{aligned}\mathbf{E}[(\mathbf{W}^\top \mathbf{W})[i, j]] &= \mathbf{E}\left[\sum_{k=1}^m \mathbf{W}[i, k] \mathbf{W}[k, j] \mathbf{1}[i, j, k \in U]\right] \\ &= \omega_i \omega_j \mathbf{E}\left[\sum_{k=1}^m \mathbf{W}[i, k] \mathbf{W}[k, j] \mathbf{1}[k \in U] \mid i, j \in U\right] \\ &= \omega_i \omega_j \mathbf{E}\left[|U|^{-2} \sum_{k=1}^m \mathbf{1}[k \in U] \mid i, j \in U\right] \\ &= \omega_i \omega_j \mathbf{E}\left[\frac{1}{|U|} \mid i, j \in U\right] \\ &\sim_m \omega_i \omega_j \mathbf{E}\left[\frac{1}{|U|} \mid U \neq \emptyset\right] = \omega_i \omega_j m^\perp.\end{aligned}$$

Using the observation that m^\perp tends to 0 as m grows, we compute asymptotically the diagonal entries as

$$\begin{aligned}\mathbf{E}[(\mathbf{W}^\top \mathbf{W})[i, i]] &= (1 - \omega_i) + \omega_i \cdot \mathbf{E}\left[|U|^{-2} \sum_{k=1}^m \mathbf{1}[k \in U] \mid i \in U\right] \\ &\sim_m 1 - \omega_i + \omega_i m^\perp \sim_m 1 - \omega_i.\end{aligned}$$

By combining the steps above, we obtain that

$$\begin{aligned}\rho(\mathbf{W}) &= \|\mathbf{E}[\mathbf{W}^\top \mathbf{W}] - \mathbf{J}\| \\ &\sim_m \left\| m^\perp \omega \omega^\top + \text{diag}(\mathbf{1} - \omega) - \frac{1}{m} \mathbf{1} \mathbf{1}^\top \right\|,\end{aligned}$$

as desired. \square

Proof of Lemma VI.2. Let τ' be the first iteration k when for every $e \in E$ there exists an iteration $j \leq k$ such that $e \in E_j$. We first prove that $\tau \leq \tau'$ by showing that $\rho_{\tau'} < 1$. For any $\epsilon \in (0, 1)$, consider a probability vector

$$\mathbf{p}' := (p_0 = 1 - \epsilon, p_1 = \epsilon/\tau', \dots, p_{\tau'} = \epsilon/\tau').$$

By taking ϵ sufficiently small, the constraint (24c) can be satisfied by \mathbf{p}' . As $\rho_{\tau'}$ is obtained by minimizing the problem defined in (24), we have

$$\rho_{\tau'} \leq \left\| (1 - \epsilon)I + \frac{\epsilon}{\tau'} \sum_{s=1}^{\tau'} \mathbf{W}_s^\top \mathbf{W}_s - \mathbf{J} \right\| =: \rho^*.$$

Denote $\frac{1}{\tau'} \sum_{s=1}^{\tau'} \mathbf{W}_s$ by $\overline{\mathbf{W}}$. By triangle inequality, we get that

$$\rho^* \leq (1 - \epsilon) + \epsilon \left\| \frac{1}{\tau'} \sum_{s=1}^{\tau'} (\mathbf{W}_s^\top \mathbf{W}_s - \mathbf{J}) \right\|$$

According to the weight assignment in Lines 6-9, every \mathbf{W}_s is symmetric and double-stochastic. Thus $\overline{\mathbf{W}}$ is also symmetric

and double-stochastic. For any double-stochastic matrix \mathbf{W} we have $\mathbf{W}^\top J = J$ and $\|\mathbf{W}\| \leq 1$, and it follows that

$$\begin{aligned} & \left\| \frac{1}{\tau'} \sum_{s=1}^{\tau'} (\mathbf{W}_s^\top \mathbf{W}_s - J) \right\| = \left\| \frac{1}{\tau'} \sum_{s=1}^{\tau'} (\mathbf{W}_s^\top \mathbf{W}_s - \mathbf{W}_s^\top J) \right\| \\ &= \left\| \frac{1}{\tau'} \sum_{s=1}^{\tau'} \mathbf{W}_s^\top (\mathbf{W}_s - J) \right\| \leq \max_s \|\mathbf{W}_s^\top (\overline{\mathbf{W}} - J)\| \\ &\leq \max_s \|\mathbf{W}_s^\top\| \cdot \|\overline{\mathbf{W}} - J\| \leq \|\overline{\mathbf{W}} - J\|. \end{aligned}$$

Moreover, by the choice of τ' , $\overline{\mathbf{W}}$ is an irreducible matrix, and thus by Perron-Frobenius theorem, $\overline{\mathbf{W}}$ has the following eigenvalues:

$$1 = \lambda_1(\overline{\mathbf{W}}) > \lambda_2(\overline{\mathbf{W}}) > \dots > \lambda_m(\overline{\mathbf{W}}) > -1,$$

and the eigenvector corresponding to the leading eigenvalue is the all-one vector $\mathbf{1}$. On the other hand, J has only 1 non-zero eigenvalue whose eigenvector is also the all-one vector $\mathbf{1}$. Hence,

$$\|\overline{\mathbf{W}} - J\| = \max(|\lambda_2(\overline{\mathbf{W}})|, |\lambda_m(\overline{\mathbf{W}})|) < 1,$$

and this implies that

$$\rho_{\tau'} \leq \rho^* \leq (1 - \epsilon) + \epsilon \|\overline{\mathbf{W}} - J\| < 1.$$

Next we prove that there exists $C > 0$ such that

$$\Pr[\tau' > Cm] \leq e^{-\Omega(m)},$$

from which the lemma follows. By assumption, there is a constant $c > 0$ such that for each $e \in E$ and every iteration k , $e \notin E_k$ occurs with probability at most $1 - c$. Then $e \notin E_j$ for any of $j = 1, \dots, t$ iterations occurs with probability at most $(1 - c)^t$. By a union bound over $e \in E$,

$$\Pr[\tau' > t] \leq m^2 \cdot (1 - c)^t \leq m^2 \cdot \exp(-ct).$$

By letting $t = Cm/c$ with C sufficiently large, the right-hand side is at most $e^{-\Omega(m)}$. \square